Materials Horizons

ROYAL SOCIETY OF CHEMISTRY

REVIEW

View Article Online
View Journal | View Issue

Cite this: *Mater. Horiz.*, 2025, **12**, 2436

Porous polymers: structure, fabrication and application

Qingxian Liu,*[ae] Jinkui Xiong,[a] Wengui Lin,[a] Jinlong Liu,[f] Yongbiao Wan,[g] Chuan Fei Guo,[d] Quan Wang*[b] and Zhiguang Liu*[c]

Received 12th November 2024,
Accepted 6th January 2025

DOI: 10.1039/d4mh01618a

rsc.li/materials-horizons

The porous polymer is a common and fascinating category within the vast family of porous materials. It offers valuable features such as sufficient raw materials, easy processability, controllable pore structures, and adjustable surface functionality by combining the inherent properties of both porous structures and polymers. These characteristics make it an effective choice for designing functional and advanced materials. In this review, the structural features, processing techniques and application fields of the porous polymer are discussed comprehensively to present their current status and provide a valuable tutorial guide and help for researchers. Firstly, the basic classification and structural features of porous polymers are elaborated upon to provide a comprehensive analysis from a mesoscopic to macroscopic perspective. Secondly, several established techniques for fabricating porous polymers are introduced, including their respective basic principles, characteristics of the resulting pores, and applied scopes. Thirdly, we demonstrate application research of porous polymers in various emerging frontier fields from multiple perspectives, including pressure sensing, thermal control, electromagnetic shielding, acoustic reduction, air purification, water treatment, health management, and so on. Finally, the review explores future directions for porous polymers and evaluates their future challenges and opportunities.

Wider impact

Porous polymers exhibit abundant structural characteristics, fabrication methods, and physicochemical properties, integrating the unique features of pore structures with the versatility of polymers. This combination makes them highly effective platforms for tackling challenges in environmental sustainability, energy, and health. Thus, exploring the structure, fabrication methods, and applications of advanced porous polymers is crucial to uncovering the fundamental relationships that guide their performance, offering valuable insights for researchers. This review provides a thorough overview of the pore structures in porous polymers—including size, connectivity, distribution, and porosity—which are pivotal not only for designing advanced materials but also for determining their application fields and efficiency. Furthermore, it systematically presents and compares various common fabrication techniques and key applications of porous polymers, offering researchers clear guidance in selecting suitable methods to achieve well-defined pore structures with optimal application potential. Additionally, this review identifies potential challenges and suggests strategies for each technique and application discussed, fostering further research and innovation.

[a] *Department of Mechanical Engineering, Shantou University, Shantou, Guangdong, 515063, China. E-mail: qxliu@stu.edu.cn*
[b] *College of Engineering, Eastern Institute of Technology, Ningbo (EIT), Zhejiang, 315000, China*
[c] *Department of Precision Machinery and Precision Instrumentation, University of Science and Technology of China, Hefei, Anhui, 230027, China. E-mail: liuzg09@ustc.edu.cn*
[d] *Department of Materials Science and Engineering, Southern University of Science and Technology, Shenzhen, Guangdong, 518055, China*
[e] *Intelligent Manufacturing Key Laboratory of Ministry of Education, Shantou University, Shantou, Guangdong, 515063, China*
[f] *Department of Mechanics and Aerospace Engineering, Southern University of Science and Technology, Shenzhen, Guangdong, 518055, China*
[g] *Microsystem & Terahertz Research Center, Institute of Electronic Engineering, China Academy of Engineering Physics, Chengdu, Sichuan, 610200, China*

1. Introduction

Porous materials, consisting of pores and a solid skeleton, are prevalent in both natural and synthetic materials.[1,2] For example, hierarchical pores in plants provide transport channels of nutrients for regular metabolism; animal bones possess numerous pores that contribute to low density and high strength, allowing them to withstand significant static and cyclic loading over extended periods. In artificial materials, previous researchers regarded pores as defects and focused on eliminating them to improve the material's mechanical properties. Until the 1930s and 1940s, scientists gradually realized that pores in materials could significantly alter their topographic

characteristics and physical properties, enabling specific functionalities that are absent in solid materials. Consequently, a research boom in porous materials ensued, emerging many unique functional porous materials.[3–6] Today, porous materials have evolved into a comprehensive scientific field with promising prospects in many emerging areas.

In the porous material family, porous polymers have attracted wide attention due to their potential to combine the merits of both porous geometry and polymers.[7,8] Firstly, the existence of pores introduces a gaseous phase into the polymers and forms additional air/polymer interfaces and channels simultaneously. This results in significant alterations in material properties, including low relative density, a large surface area, and high interconnectivity.[9–11] Secondly, porous polymers have the advantages of being lightweight, flexible, and corrosion-resistant due to the polymer skeleton composed of light elements such as carbon, hydrogen, and oxygen, as well as the nature of covalent bonds. Meanwhile, porous polymers can be easily processed because of their inherent polymeric characteristics such as solubility, low melting point, and machinability. Numerous mature and cost-effective manufacturing methods based on solution casting,[12] melt molding,[13] and machining,[14] have been successfully developed. These methods offer increased opportunities for identifying a suitable shaping approach that aligns with the requirements of rational materials design. Thirdly, numerous general polymers, engineering polymers, and biopolymers can be used to construct porous materials.[15–18] The availability of diverse materials is both sufficient and necessary to meet the application requirements in various scenarios. Benefiting from sufficient processing methods and materials, porous polymers exhibit flexibility and diversity in forms, including textiles, papers, sponges, fiber membranes, and so on. In addition, inorganic fillers such as graphene, carbon nanotubes (CNTs), metal, MXene, and silica, have been compounded with polymers to engineer composite porous materials,[19–21] further enriching the structures and

Qingxian Liu

Qingxian Liu is an assistant professor in the Department of Mechanical Engineering at Shantou University. He received his PhD degree in the Department of Mechanics and Aerospace Engineering from Southern University of Science and Technology, China. His scientific interests include the design and fabrication of porous polymers and their application in flexible electronics, absorption and separation membranes, and so forth.

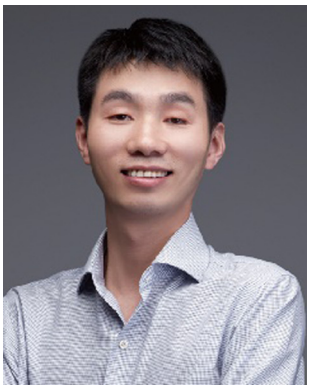

Chuan Fei Guo

Chuan Fei Guo is a professor in the Department of Materials Science & Technology, Southern University of Science and Technology, China. He received his PhD degree from the National Center for Nanoscience and Technology, (NCNST), Chinese Academy of Sciences, China. From 2011 to 2016, Dr Guo worked as a postdoctoral fellow and research associate at Boston College and the University of Houston. He is an influential scholar in flexible electronics and advanced manufacturing. He serves as an editor for Materials Today Physics.

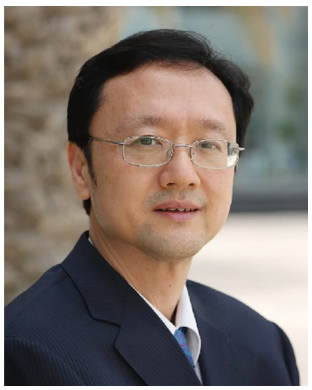

Quan Wang

Quan Wang received his PhD degree in Solid Mechanics at Peking University in 1994. He is an influential scholar in the research areas of energy harvesting, smart materials, and nanotechnology. He was inducted into the Canadian Academy of Engineering and the Royal Society of Canada in 2015 and 2016 respectively.

Zhiguang Liu

Zhiguang Liu is a Professor and PhD Supervisor in the Department of Precision Machinery and Precision Instrumentation, University of Science and Technology of China (USTC). He received his bachelor's degree from the USTC's Special Class for the Gifted Young and his PhD from the Institute of Physics, Chinese Academy of Sciences. His research interests focus on exploring the physico-chemical interaction mechanisms at the micro- and nanoscale, advancing state-of-the-art three-dimensional micro- and nanofabrication technologies, and addressing scientific challenges in optics, mechanics, and biomedicine.

physicochemical properties of the porous polymer family. Such unique feature makes porous polymers essential multifunctional platforms for addressing environmental, energy, and health challenges that emerge in the advancement of human society.[22–25]

The ability of porous polymers to achieve the desired function in a particular application is closely related to several factors below. One of them is the pore structures, including porosity, interconnectivity, and pore's size, shape, and distribution;[26–29] For example, high-porosity sensing layers in pressure sensors bring low modulus, resulting in significant deformation under external force. This phenomenon effectively amplifies the variation of sensing signals and enhances the sensitivity of the pressure sensors;[30] nanoscale pores can effectively restrict heat transport inside the materials, thereby enhancing its thermal insulation capability;[31] porous membranes composed of ultrafine nanofibers reduce the mass-transfer resistance and increase interaction with target molecules, which is a promising material for highly efficient air purifiers;[32] hierarchal porous structure with a gradient in pore size is particularly important for water purification as it combines high filtration efficiency with high flux.[33] The second aspect is the physicochemical properties that come from the intrinsic polymer skeletons or decorated pore walls. The

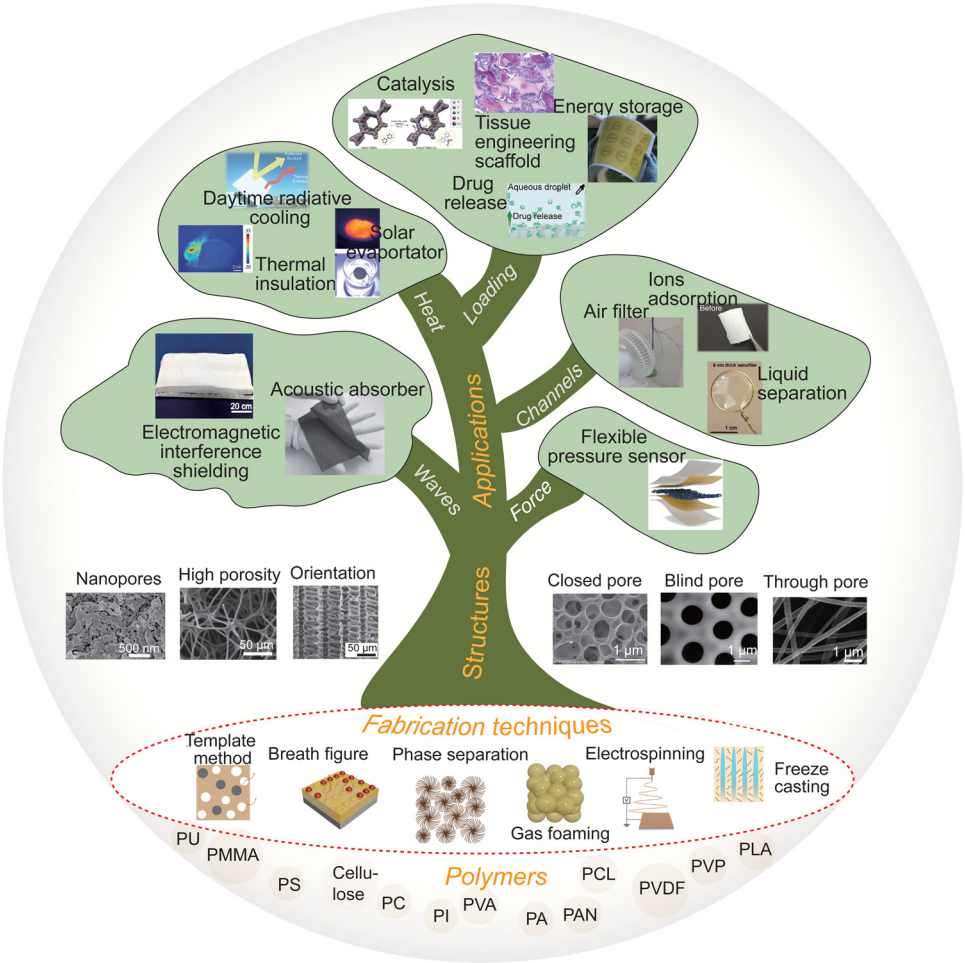

Fig. 1 Overview of porous polymers including their common materials, major fabrication techniques, structures, and leading-edge applications. Image for "Orientation": reproduced with permission.[39] Copyright 2007, American Ceramic Society. Image for "Flexible pressure sensor": reproduced under the terms of the CC-BY Creative Commons Attribution 4.0 International license (https://creativecommons.org/licenses/by/4.0).[30] Copyright 2022, The authors, published by Springer. Image for "Acoustic absorber": reproduced with permission.[40] Copyright 2021, Elsevier. Image for "Electromagnetic interference shielding": reproduced with permission.[41] Copyright 2013, WILEY-VCH. Image for "Thermal insulation": reproduced with permission.[42] Copyright 2018, WILEY-VCH. Image for "Daytime radiative cooling": reproduced with permission.[43] Copyright 2018, American Association for the Advancement of Science. Image for "Solar evaporator": reproduced with permission.[44] Copyright 2021, American Chemical Society. Image for "Catalysis": reproduced with permission.[45] Copyright 2019, American Chemical Society. Image for "Tissue engineering scaffold": reproduced with permission.[46] Copyright 2007, Elsevier. Image for "Energy storage": reproduced with permission.[47] Copyright 2019, The Authors, published by Springer Nature. Image for "Drug release": reproduced with permission.[48] Copyright 2023, Wiley-VCH. Image for "Air filter": reproduced with permission.[49] Copyright 2015, Macmillan Publishers Limited. Image for "Liquid separation": reproduced with permission.[50] Copyright 2015, American Association for the Advancement of Science. Image for "Ions adsorption": reproduced under the terms of the CC-BY Creative Commons Attribution 4.0 International license (https://creativecommons.org/licenses/by/4.0).[51] Copyright 2021, The Authors, published by Springer Nature.

constituent units of polymer possess rich functional groups, allowing the construction of unique physical/chemical characteristics through presynthetic and postsynthetic processes. Typically, grafted ion-exchange groups on the hydrophobic skeletons of highly porous polymer is an effective method to fabricate new ion-exchange membranes with high capacity and fast kinetics.[34] As for the third aspect, it can be called the composite type in which extra functional fillers are blended in the polymer or appended on the pores. For example, when porous polymers are combined with resonance nanomaterials, they exhibit significant low-frequency acoustic absorption, offering a potential solution to the challenges of thickness and inefficiency associated with conventional sound absorbers.[35] Moreover, porous composites consisting of polymers and conductive materials such as metal or carbon-based conductors incorporate conductive networks, chemical stability, and multifunctionality. These optimized porous composites combine the advantages of polymers and functional fillers, providing increased opportunities to complement porous polymers in various fields, especially as active electrode materials for heat treatment, electromagnetic shielding, and energy storage.[36–38]

In this review, we focus on the design and fabrication of the functional structure of porous polymers for promising applications. It begins by categorizing the structures of porous polymers and their mainstream fabrication techniques, and then introduces the fundamental principles, characteristics, and scope of each technique. Subsequently, the recent advancements in the application of porous polymers are discussed, evaluating their properties related to mechanics, heat transfer, wave propagation, molecular absorption/separation, and load capability. The discussion emphasizes developments in popular research fields such as flexible pressure sensing, thermal management, electromagnetic shielding, noise reduction, adsorption separation, drug releasing, tissue engineering, and so forth. Fig. 1 illustrates the overall framework of the porous polymer system discussed in this review. Finally, we discuss the challenges and perspectives for emerging porous polymers and composite materials, which will help others understand their nature and create advanced polymer-based porous structures.

2. Structures of the porous polymers

Porous polymers display abundant structures and functionalities based on pore geometries and skeleton features. The size, connectivity, distribution, and proportion of pores play crucial roles in determining the physical properties of these materials. It is generally agreed that the size of pores can be classified into micropores (<2 nm), mesopores (2–50 nm), and macropores (>50 nm) according to the International Union of Pure and Applied Chemistry. In fact, a significant proportion of porous polymers possess microscale and millimeter-scale pores, some even large enough to be visible to the naked eye. Given the order of magnitude difference in size compared to nanoscale pores, we redefine the pore with a size ranging from 1–1000 μm size as micron pores and the pore size up to 1 millimeter or above as large pores, as demonstrated in Fig. 2a. These diverse sizes of pores offer distinct structural advantages. For instance, micropores and mesopores contribute to high specific surface area based on the deduced relation expression $S_V = 6V_p/D_p$, S_V is the specific surface area, V_p is the material porosity, and D_p is the feature size of pore. The equation presents that micropores or mesopores with diameters ranging from a few to tens of nanometers result in a large specific surface area at a fixed porosity. Such as the specific surface area of MOF-210 with micropores reaches up to 6240 $m^2\ g^{-1}$, which was previously a record.[52] High specific surface area provides numerous reactive sites, size-selectivity for molecules, and a substantial interfacial area. These characteristics are widely utilized in absorption, separation, and catalysis;[53] According to the Kozeny–Carman equation,

$$K = \frac{V_p^3}{(1 - V_p)^2} \cdot \frac{D_p^2}{m}$$

where m is a constant related to the geometry of the material. we can clear see that the permeability (K) of porous materials is proportional to the square of the pore's diameter. Therefore, macropores usually offer relatively unrestricted channels for the diffusion and permeation of small molecules, thereby mitigating the diffusion limitations in purely micro-/mesoporous materials;[54] an important point of the micron pore and large pore lies in their ability to provide ample storage and growth space for cells or tissues, which is crucial in tissue engineering scaffolds.[55] Moreover, composite sizes such as meso-macro, micro-macro, and other combinations also often appear in the materials fabricated by combining various techniques,[56] compensating for the limitations of single-size pores and greatly expanding the material's geometry. In addition, these composite pore sizes can substantially boost performance in controlling continuous matter waves and mechanical waves, including sound waves, electromagnetic waves, and optical waves, by matching a wider range of wavelengths.[57,58]

Furthermore, pores can be classified into open (including blind pores and through pores) and closed structures by their connectivity, as shown in Fig. 2b. Through pores with interconnected channels that allow the dispersion of gaseous or liquid phases are indispensable in the applications related with exchange, absorption, separation of substances. However, the presence of through pores may compromise the mechanical strength of materials and raise concerns about dimensional stability. The mechanical behaviors of the through pore structure, such as uniaxial compression, elastic buckling, brittleness and plastic failure have been systematically researched by Gibson and Ashby.[62] Blind pores are regarded as semi-open structures, known for their role as an effective template to reprint micro-convex structures in pressure sensors or optical devices. When the pore wall is intact and able to hold the gaseous phase, it prevents interconnections with neighboring pores and forms an independent closed pore. Obviously, due to the channel-less and confined space, this structure is

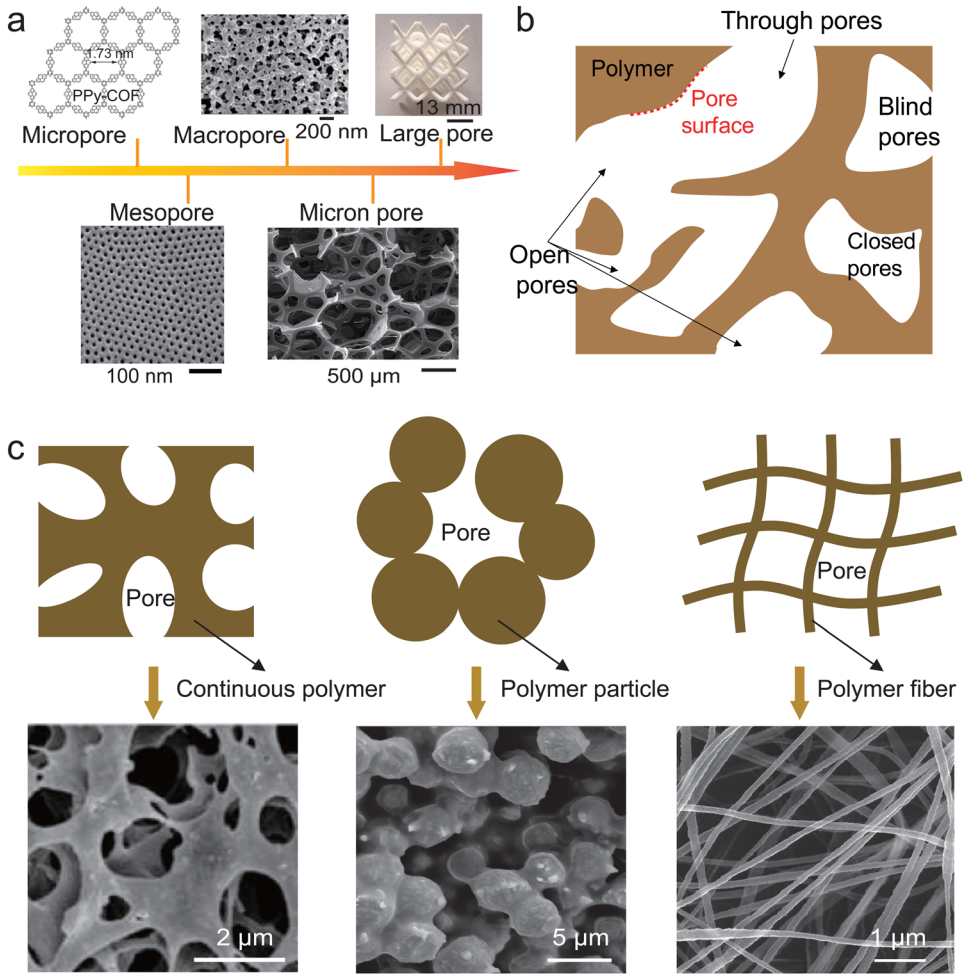

Fig. 2 Categories and forms of porous polymers. (a) Size features of porous polymer, including micropore (reproduced with permission.[59] Copyright 2009, Wiley-VCH), mesopore (reproduced with permission.[60] Copyright 2010, American Chemical Society), macropore, micron pore and large pore. (b) Illustration of pore geometry and framework structure of porous polymers in cross-section. (c) Three structural forms of solid skeletons in porous polymers, which are continuous polymer (SEM image is reproduced with permission.[61] Copyright 2014, American Chemical Society), particles, and fibers, respectively.

unsuitable as a functional platform in the related fields of transport, catalysis, loading, and so on. However, closed-pore types provide effective support in transport packaging due to their compression recovery. Meanwhile, they are increasingly being used for caulking plates due to their strong waterproof performance, high recovery rate, and anti-penetration performance. Furthermore, the porosity, defined as the volume ratio of pores, is another crucial structural characteristic of porous polymers. High porosity can significantly reduce the density and elastic modulus of materials, as detailed analysis in Section 4.1. For example, our previous experiments showed that the elastic modulus of non-porous PU is ~6.5 MPa, while the modulus significantly decreased to ~3.4 kPa in porous PU with 98.8% porosity.[30] The reduction in density and modulus are particularly advantageous for the development of lightweight and flexible devices. In addition, other physical properties of materials, such as specific heat and thermal conductivity, both decrease with increasing porosity. The distribution of pores, such as the location of each pore in the substrate, also requires attention because of its influence on heat transfer, electron and ion transport, mass loading, and diffusion. Such as aligned porous structures are proven to be effective for heat manipulation because they can improve the multiple reflectivity of infrared radiation by increasing the density of solid–gas interface perpendicular to the thermal gradient.[63] Apart from pore structure, the detailed pore chemistry is another crucial role.[64] The pore surfaces provide natural sites for functional modifications using functional monomers or post-modification processes, greatly expanding the properties and potential applications of porous polymers.

Another key component in porous polymers is the solid polymer skeleton, which also presents several typical types such as continuous matrix, stacked particles, and fibers (as shown in Fig. 2c). The formation mechanism of a continuous skeleton is similar to subtractive manufacturing, which removes parts of the material to produce desired pores. The topologies of this skeleton are determined by pore structures that can be spherical, network-type, cellular, tubular, and other forms which

may be either disordered or ordered arrays. Another skeleton type is formed from densely packed polymer particles, including microspheres, microsheets, or other shapes of particles. Generally, these structures occur during the phase transformation of crystalline polymers as a result of polymer chain folding. However, it is difficult to obtain regular pores because the position of particles cannot be precisely targeted during the crystallization process. Besides the particles, stacked fibers are also a very common and useful form in porous polymers, easily obtained through spinning techniques.[65] Compared to microparticles, nanofibers possess higher aspect ratios and then results in superior flexibility, which is essential for wearable functional devices or electronic skin. It should be pointed out that the prominent feature of the stacked form is the high interconnectivity of pores, with almost no blind or closed pores. This is because the particles or fibers with large curved structures are difficult to form tight and seamless accumulations with each other. Also, the mechanical strength of stack-based porous polymers is relatively inferior to that of continuous skeletons, and researchers generally employ interfacial crosslinking to address this limitation. In addition, the hollow core–shell structure within microspheres or fibers is also a common form in porous polymers, widely used in thermal insulation, catalysis, microelectronic devices, and so on.

Overall, the pores and polymer skeletons are inseparable components that together construct a rich and diverse family of porous polymers, and we should consider them together in design and production. Such unique characteristics of porous polymers provide a multifunctional platform to open up avenues for many application fields.

3. Fabrication of the porous polymers

Polymers have excellent moldability, which is one of the main reasons for their widespread research and use, and this characteristic is well inherited in porous polymers. According to the original aggregation morphology of macromolecular chains, the processing mode for polymers includes three types: dissolving in a good solvent to form a solution; melting by heating; and direct structuring by machining. Over the last few decades, numerous techniques have been developed to fabricate desired porous polymers by using these types, allowing for the structural control of porous polymers across various dimensions. It is a significant factor in the boom of porous polymers and provides adequate options for the simple and scalable production of high-performance materials. The term ''polymer solution'' refers to the uniform dispersion of polymer molecules in a solvent, commonly utilized in the production processes of porous polymers such as solution electrospinning,[66] breath figuring,[67] freeze-drying,[68] soft templating,[69] self-templating,[70] and phase separation.[71,72] Melt processing techniques including gas foaming,[73] melt spinning,[74] and melt 3D printing[75] are considered to be more environmentally friendly due to the formation of a machinable polymer fluid by heating rather than organic solvents. Laser cutting is a typical machining method that does not need to change the original aggregation morphology of polymeric chains[76] and allows for precise control of pore structure by a preset program. Each of these procedures has particular advantages and disadvantages, which can be used to control the pore structures with innovative properties targeting selected applications, as shown in Fig. 3.

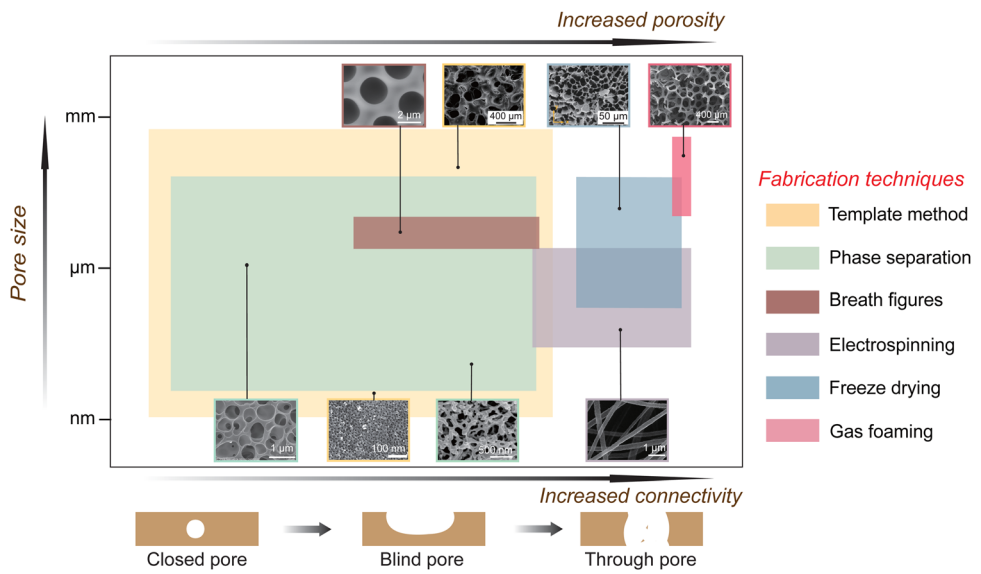

Fig. 3 The corresponding relationship between the various preparation techniques of porous polymers and the resulting pore structures. Herein, the area covered by each technique represents only the range of pore structures that it may obtain, and this representation of porosity does not exhibit a clear proportional relationship with connectivity. Note that the gas foaming can also prepare closed pore while preserving high porosity. The SEM image of the nanopores fabricated by template method (scale bar 100 nm) is reproduced with permission.[77] Copyright 2016, WILEY-VCH. The SEM image of the micrometer pores fabricated by template method (scale bar 400 μm) is reproduced with permission.[44] Copyright 2021, American Chemical Society. The SEM image of the anisotropic pores fabricated by freeze drying is reproduced under the terms of the CC-BY Creative Commons Attribution 4.0 International license (https://creativecommons.org/licenses/by/4.0).[78] Copyright 2022, The Authors, published by Springer Nature.

To help researchers better understand the mainstream fabrication processes of porous polymers, the working mechanisms, structural characteristics of obtained materials, and scope of applications for several techniques frequently used are reviewed and summarized below.

3.1. Electrospinning

Electrospinning is a continuous, economical, and versatile technique for producing micro/nanofiber-based porous polymers. During the electrospinning process, a viscous polymer solution is stretched and deformed into a Taylor cone at the nozzle tip due to a strong electrostatic field. The charged droplet will be ejected once its Coulombic repulsive force exceeds its surface tension, and then the liquid jet is elongated and the solvent evaporates to form solidified polymer fibers. Finally, a porous membrane with highly interconnected pores is formed on a collector through the natural accumulation of these solidified fibers,[79] as illustrated in Fig. 4a. The structural parameters of the fiber-based porous polymers, including porosity, morphology, and specific surface area, can be easily designed by adjusting the process conditions such as voltage, temperature, humidity, distance between the nozzle and

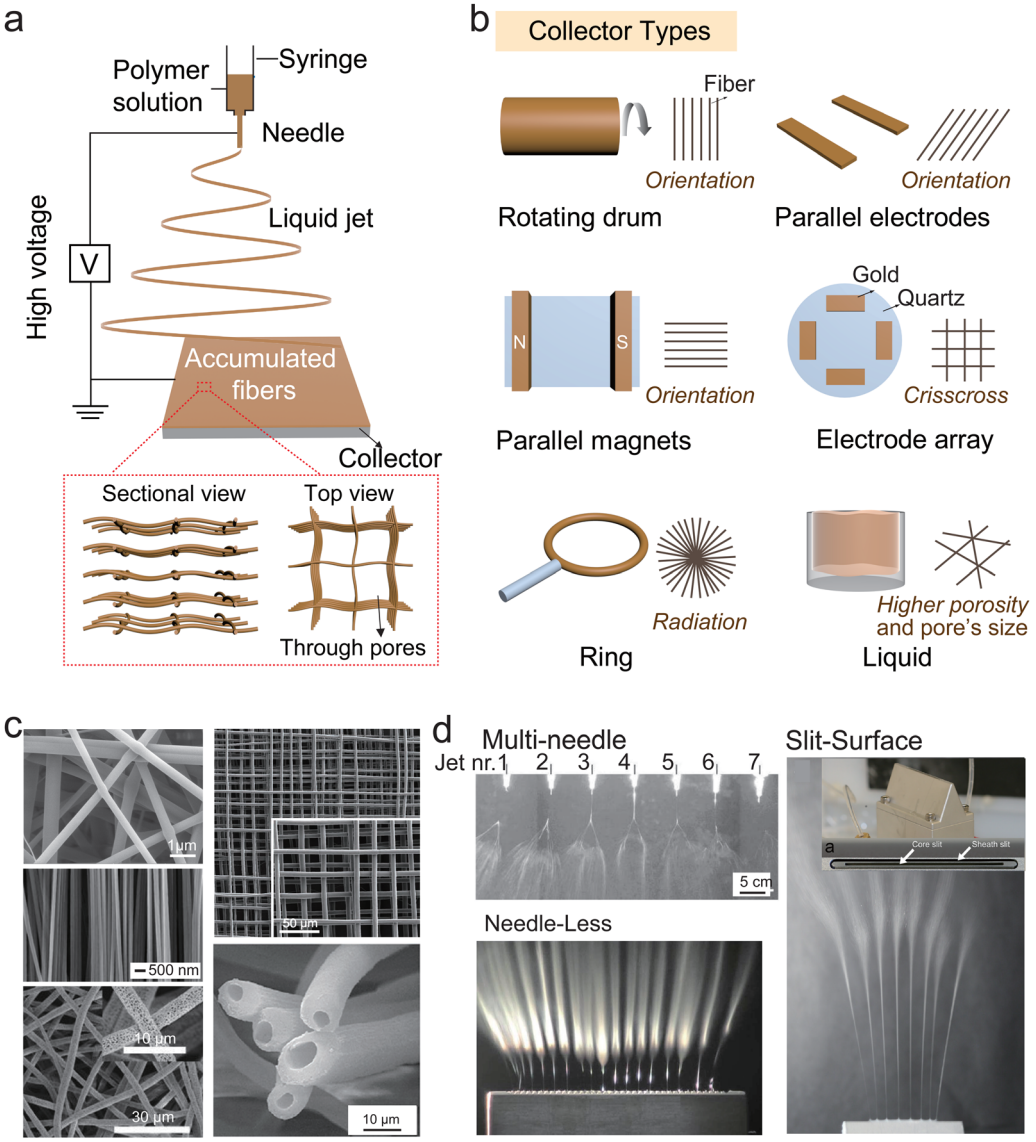

Fig. 4 Fiber-based porous polymers fabricated by using electrospinning technique. (a) Schematic of a typical electrospinning equipment on laboratory scale, the pores in this fibrous film present high connectivity due to being formed by fibers stacking. (b) Schematic of the various collectors for electrospinning including rolling drum, parallel electrodes, parallel magnets, electrode array, ring, and liquid. (c) Microstructural forms of the porous polymer including random, orthogonality (reproduced with permission.[83] Copyright 2011, Wiley-VCH), orientation (reproduced with permission.[84] Copyright 2003, American Chemical Society), surface pore (reproduced with permission.[85] Copyright 2015, Elsevier) and core–shell structure (reproduced with permission).[86] Copyright 2012, Elsevier. (d) Photographs of the multi-needle (reproduced with permission.[87] Copyright 2005, Elsevier), needle-less (reproduced with permission.[88] Copyright 2008, American Institute of Physics), and slit surface (reproduced with permission.[89] Copyright 2015, Public Library of Science) from the polymeric solution system in electrospinning apparatus.

collector, and the solution composition during electrospinning.[80] When the polymer is poor solubility (such as polypropylene (PP), polyethylene (PE), and polyvinyl chloride (PVC)) or requires a toxic solvent, melt electrospinning (a technique to produce fibers by using polymer melts) can be adopted instead of solution electrospinning, offering a promising supplemental method for producing fiber-based materials.[81,82]

The pore structure of fibrous membranes is closely related to the diameter and packing arrangement of the fibers. Smaller fiber diameters result in smaller pore sizes and higher specific surface areas due to a greater number of fibers being stacked under the same porosity and thickness. Moreover, the shapes and materials of collectors significantly affect the distribution of the electric field, offering diverse options for achieving specific pore structures.[90] It is well-known that conventional plate-metal collectors will result in the random accumulation of fibers, typically forming irregular pores.[91] To achieve specific structures, several modified collectors for electrospinning have been reported, and their schematic and corresponding arrangement of fibers as shown in Fig. 4b. The rolling drum, parallel electrodes, and parallel magnetic all cause directional alignment of nanofibers to obtain anisotropic pores;[92] electrode array can induce fibers to arrange in a cross pattern at specific angles, forming a regular mesh pores;[93] ring electrode induces scattering of nanofibers from the center of the circle outward, leading to radial pores;[94] solvents such as water or ethanol as collectors can increase the dispersion of fibers and significantly reduce their adhesion, thereby increasing pore size and porosity.[95] In addition, the pores can form on the surface of ultrafine fibers when adopt highly volatile solvents or in a high-humidity atmosphere.[85] Fig. 4c presents several representative morphologies of fiber-based porous materials, including random, orthogonal, oriented, multistage, and core–shell structures. These structures have attracted considerable attention in filtration, thermal management, drug release, and wearable electronics.[96–98] However, since the driving force of electrospinning is the electric field, high voltage is necessary and brings a potential safety hazard. Furthermore, electrospinning suffers from low efficiency in fiber production, which is an obvious limitation of this technique. To overcome the challenge of large-scale production, multi-needle and needleless (jetting from the free liquid surface) spinning techniques (as shown in Fig. 4d) have been developed to improve the production efficiency of porous nanofiber membranes.[88,89,99] Further research is expected to yield more favorable outcomes and ultimately facilitate the production of functional porous nanofibers through advanced electrospinning techniques.

3.2. Breath figures

Breath figures (BFs) method, also known as water droplet patterning method, involves the self-assembly of moisture into ordered arrays within a polymer casting solution. The procedures of BFs include the following stages: (1) evaporation of the organic solvent with a low boiling point results in the cooling of the polymer solution; (2) water vapor condenses onto the cold solution surface, forming water droplets; (3) continuous condensation of water vapor promotes the growth and self-organization of water droplets into an ordered array; (4) subsequent the organic solvent and water droplets evaporate completely, leaving solidified porous polymers.[100–102] The schematic of this process is shown in Fig. 5a. Compared to other templating and lithography techniques, the BFs method does not require an additional step to remove the template because of evaporating spontaneously of droplets. Therefore, this method provides opportunities to fabricate porous polymers with ordered pores through simple and cost-efficient operation.

The process of BFs is non-isothermal and nonequilibrium, exhibiting a greater degree of empiricism. Published articles have reported the influence of polymer type, solvent type, humidity, temperature, airflow velocity, and substrates on pore formation and morphology.[107–109] Fig. 5b shows the variations in pore structure among three BFs prepared in methanol, ethanol, and water atmospheres.[103] These structural differences primarily stem from the variations in interfacial tension between the droplet and polymer solution. In addition, the substrate on which deposited the polymer solution also plays a very important role in the regularity and ultimate quality of the pore array. Generally, coasting polymer solution on a solid substrate such as glass and metal could lead to a dense polymer layer on substrate-contacting side, forming a typical blind-pore structure.[110] However, when the polymer solution is cast onto a non-solid substrate such as water that allows the further falling of the liquid droplets, through pores can be induced. The key factor for generating through pores is that the pressure difference induced by the surface tension of the substrate liquid across the meniscus should exceed the critical pressure at which the thin polymer film ruptures. Fig. 5c shows the illustration of the formation of through pores and curves of differential pressure and critical pressure.[104] It is worth noting that the BFs technique can overcome the limitation of curved fabrication due to the flexibility of water droplet condensation, providing a facile strategy to fabricate micropores on non-planar substrates (Fig. 5d).[111] Furthermore, hierarchically ordered pores can be also prepared by BFs with the assistance of templates. For example, when a grid template is placed on the surface of an evaporating solution, the BFs only appear in the mesh space of the grid, as shown in Fig. 5e.[106] Although it is difficult to precisely predict the formation of pores and produce nanoscale pores using the BFs method, it remains an effective approach for creating ordered porous polymers and has strongly advanced this field.

3.3. Gas foaming

Gas foaming is a practicable technique to produce porous polymer foams by introducing and expanding a blowing agent within softened or molten polymers. This process effectively transforms unstable foaming into a stable and industrially scalable product.[112] Gas foaming involves a complex thermodynamic process, including the admixing of blowing agents and precursors, foaming (bubble nucleation and growth), stabilization, and solidification, the schematic of the blowing

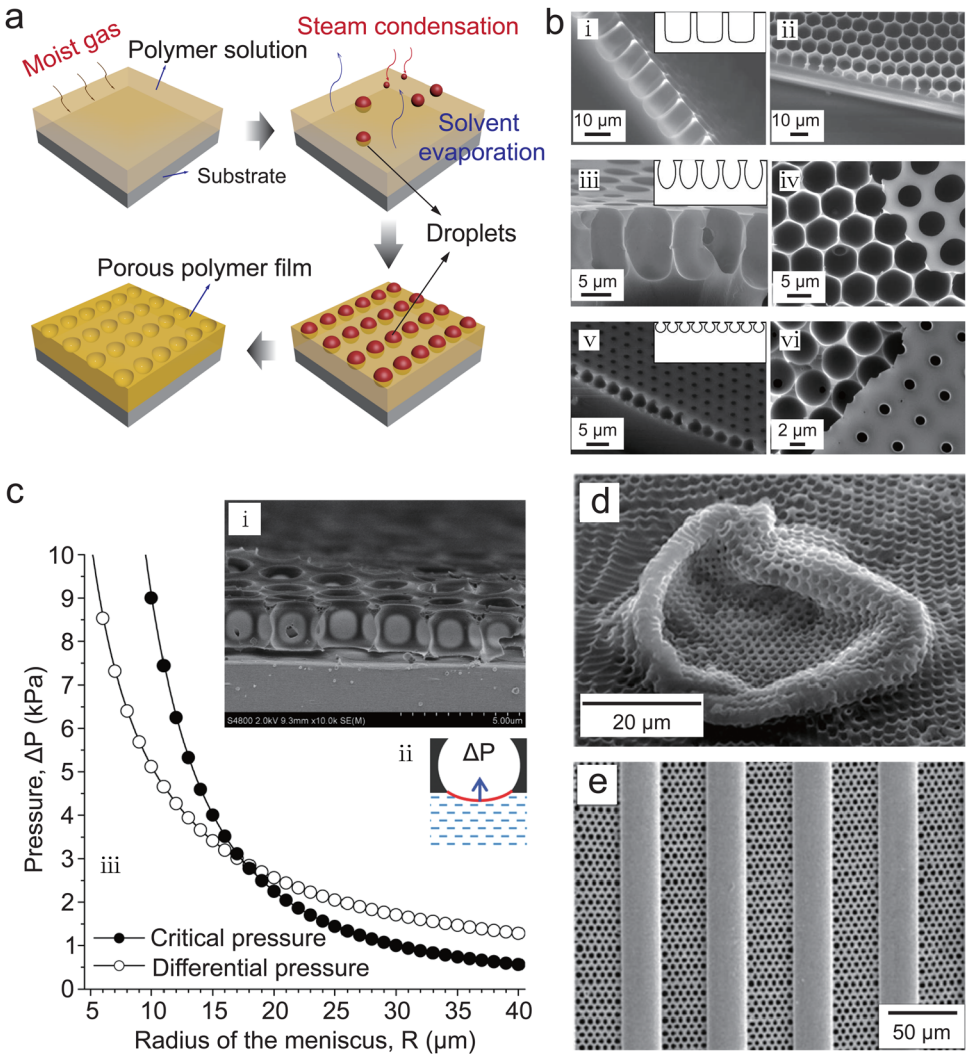

Fig. 5 Ordered porous polymers fabricated by using breath figures. (a) Schematic of honeycomb polymer films prepared by BFs. (b) Morphologies of the pores in polymer films prepared under methanol and ethanol vapor atmospheres. Reproduced with permission.[103] Copyright 2013, Royal Society of Chemistry. (c) (I) Through-pores polymers prepared by using water as a soft substrate. (II) Illustration of the formation of through pores. (III) Calculated curves of differential pressure and critical differential pressure *vs.* the radius according to the formula of differential pressure. Reproduced with permission.[104] Copyright 2012, American Chemical Society. (d) Morphologies of a porous film fabricated by BFs on non-planar substrate. Reproduced with permission.[105] Copyright 2013, Royal Society of Chemistry. (e) A hierarchical structure fabricated by placing a parallel grating on the surface of the evaporating solution. Reproduced with permission.[106] Copyright 2007, Wiley-VCH.

process is shown in Fig. 6a.[113] Foaming is crucial to guide the pore structure at micro-scales to macro-scales, which is essential to produce desired porous foams. Based on the classical nucleation theory, the free energy barrier reaches its peak when the radius of gas (R) equals the critical radius (r^*) (an nucleus should have before it can grow to become a stable bubble). Below this r^*, the nucleus is unstable and can redissolve into the melt; above this radius, the nucleus is stable and then continues to grow (Fig. 6b).[114] The critical radius, nucleation rate, and number of pores of bubbles can be resolved based on the change in critical Gibbs free energy during the nucleation process. According to the thermodynamic energy conservation theorem,[115] the change in total Gibbs free energy (ΔG) of the gas and polymer system during blowing is: $\Delta G = -(4/3)\pi R^3 \Delta P + 4\pi R^2 \gamma$, where ΔP is the pressure difference between inside and outside of bubble; γ represents the gas-melt interfacial tension. Since $\partial(\Delta G)/\partial R = 0$ for the critical bubble nucleus in the foaming process, it can be derived that the radius R of the critical bubble nucleus: $R = 2\gamma/\Delta P$. In addition, the static nucleation rate J of the bubble can be expressed as: $J = B_0 f_0 \exp(-\Delta G/k_B T)$, where B_0 is gas concentration; k_B denotes Boltzmann's constant; T is the foaming temperature; and the number of pores (N_{pore}) obtained from the integration of the rate of bubble nucleation over the foaming time is:

$$N_{pore} = \int_0^f J d$$

where f is the frequency factor of the gas nucleation. So theoretically, increasing the pressure of foaming can effectively reduce the energy barrier for nucleation and nucleation radius

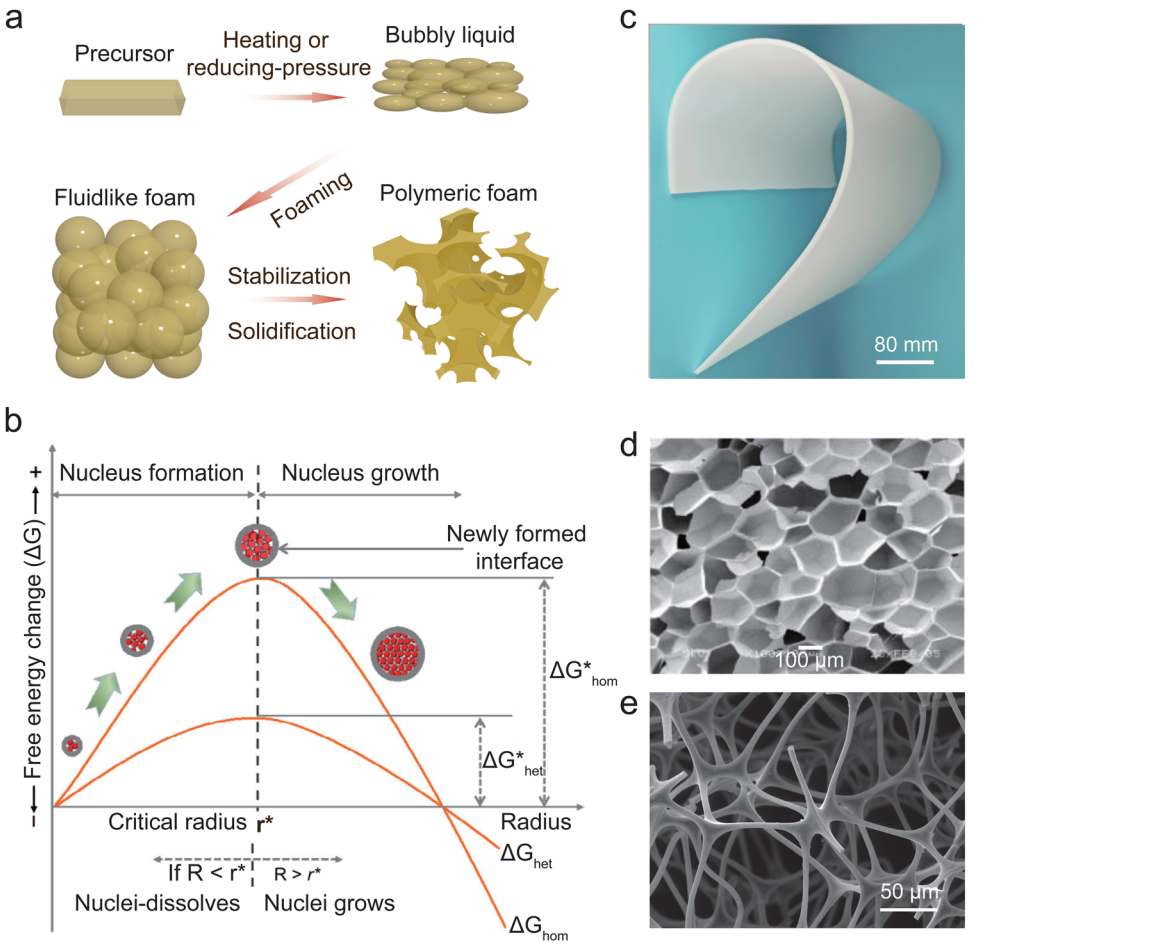

Fig. 6 Gas foaming to fabricate porous polymer foams. (a) Schematic of a typical blowing process. (b) Bubble nucleation and growth as a function of free energy. Reproduced with permission.[114] Copyright 2015, Elsevier. (c) Photo of commercial melamine foam fabricated by blowing technique. (d) and (e) Morphologies of a closed-pore structure (d) (reproduced with permission.[118] Copyright 2007, Elsevier) and an open-pore structure (e).

of bubbles, thus increasing the number of pores. Additionally, higher gas concentration and foaming temperature can also lead to an increased number of bubbles, ultimately regulating pore structure.[116,117] Generally, the gas foaming method produces polymer foam with over 98% porosity and high mechanical strength, which is a huge highlight and provides a facile and simple route to achieve highly porous materials.

At present, the theoretical and technological research on the foaming technique has greatly advanced, successfully fabricating industrial-scale products such as polyurethane foam and melamine foam (Fig. 6c). Through pores and closed pores (Fig. 6d and e) are two main structural forms in the foam fabricated by gas foaming.[119] Closed-pore foams present excellent cushioning capacity for resisting external disturbance. Through-pore foams have higher absorption and permeability for gases and liquids, lower insulation to heat or electricity, as well as the potential ability to absorb and damp sound. And yet the through pores are detrimental to the dimensional stability and mechanical properties of the materials. In addition, the physicochemical properties of porous foams can effectively improve by blending multiple polymers due to the synergistic effects between materials. Such composite polymer foams with tailor-made properties offer a novel approach to producing high-performance materials for construction, transportation, sports, medical, aerospace, and military applications.

3.4. Phase separation

The phase separation method, introduced by Loeb and Sourirajan in 1963,[120] has been widely studied in the fabrication of porous polymers owing to adaptable production scales and cost-effectiveness. In this approach, a thermodynamically stable polymer solution becomes unstable upon the addition of non-solvent or removal of thermal energy, resulting in a reduction of free energy and the formation of rich and poor polymer phases. The rich phase serves as the framework for the porous material during the curing process, while the removal of the poor phase results in pores formation.

Phase separation of polymer solutions can be categorized into non-solvent induced phase separation (NIPS) and thermally induced phase separation (TIPS) depending on the driving conditions.[121,122] NIPS is a ternary composition in which a polymer solution is immersed in a non-solvent to produce a

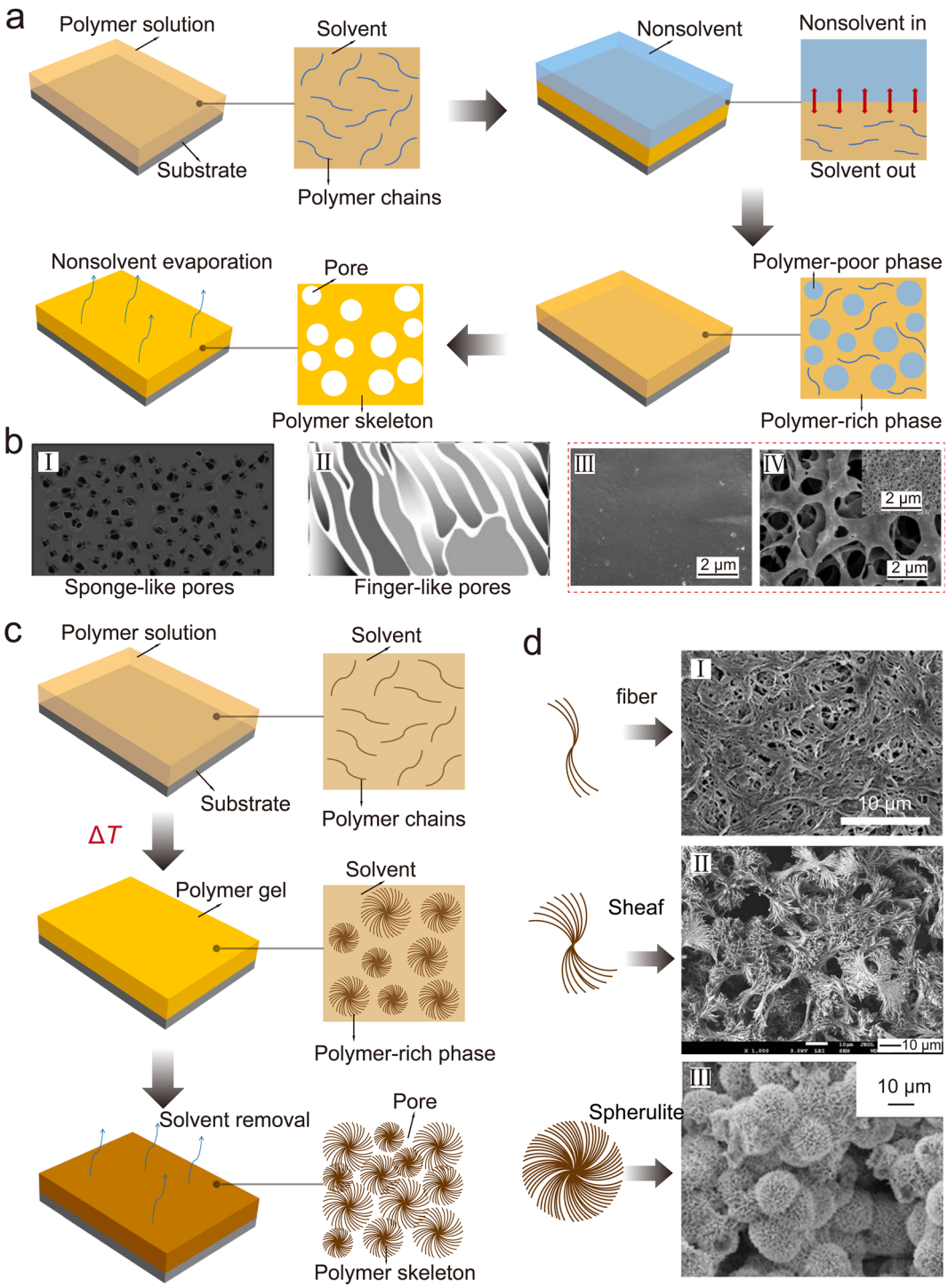

Fig. 7 Phase separation method to fabricate porous polymers. (a) Schematic of the fabrication process of porous polymer membrane by NIPS. (b) Morphologies of various porous polymers obtained by using NIPS: (I) and (II) sponge-like pores and figure-like pores, respectively. Reproduced with permission.[123] Copyright 2011, American Chemical Society; PLA films that are without (III) and with (IV) silica nanoparticles. Reproduced with permission.[61] Copyright 2015, Elsevier. (c) Schematic of the fabrication process of porous polymer by TIPS. (d) The growth process of spherulites from small sheaves to larger sheaves and then to spherulitic particles and their corresponding morphology. (I) fibers (reproduced with permission.[125] Copyright 2015, Royal Society of Chemistry); (II) sheaves (reproduced with permission.[126] Copyright 2014, Wiley Periodicals, Inc.); (III) spherulites (reproduced under the terms of the CC-BY Creative Commons Attribution 4.0 International license (https://creativecommons.org/licenses/by/4.0).[127] Copyright 2021, The authors, published by MDPI).

porous structure by displacing the solvent with the non-solvent, as shown in Fig. 7a. In this process, the pore morphology is determined by liquid–liquid phase demixing. When the polymer solution solidifies slowly in the non-solvent bath, the

resulting membrane exhibits a sponge-like substructure, as demonstrated in Fig. 7b (image I). Conversely, rapid polymer precipitation upon immersion generally results in a membrane with a finger-like pore substructure (Fig. 7b(II)).[123] Furthermore, the solution-phase separation induced by a nonsolvent usually results in membranes with dense skins on the upper surface and closed pores in the bulk, particularly in high-concentration solutions.[124] Adding inorganic nanoparticles to the polymer solution is an efficient strategy that can promote pore connectivity and improve porosity, providing a facile route to achieve highly porous membranes. The key to this strategy is that the added nanoparticles can form interactions and associations with the solvent in the polymer solution, thereby effectively preventing the contraction caused by the polymer matrix and promoting pore interconnectivity. Images III and IV of Fig. 7b demonstrate that the pore connectivity of porous polylactic acid (PLA) membranes is dramatically improved by introducing silica nanoparticles.[61]

For most semi-crystalline and crystalline polymers, phase separation can be achieved by thermally induced crystallization, as shown in Fig. 7c. This method relies on the quenching of the polymer solution below the binodal solubility curve and inducing solid–liquid separation. Due to the folding of macromolecule chains during the crystallization process, the material possesses highly interconnected pores and avoids a dense epidermal layer. In addition, the pore morphology can be easily modulated by adjusting the quenching temperature and rate, as well as the concentration of the polymer solution. Lower temperatures result in a higher rate of solvent nuclei formation and restricted crystal growth, leading to the formation of numerous small crystals, lamellae, or sheaves and a smaller pore size. Higher temperatures limit the nucleation rate and accelerate crystal growth, leading to the development of spherulites and larger pores. A concise formation process of the porous semi-crystalline polymer by TIPS is illustrated in Fig. 7d.[125–127]

In short, the phase separation method is a convenient and straightforward technique for producing porous polymers. allowing for a flexible selection of materials and preparation parameters. This facilitates the achievement of desired pore structures, making it adaptable for various environmental applications and providing robust structural and environmental adaptability.

3.5. Freeze drying

Freeze drying, also known as ice templating, is a typical technique used to produce biomimetic porous polymers across multiple length-scales. During the freeze-drying process, phase separation occurs as the solvent (usually ice) crystallization and growth in a specific direction. The solidified solvent is subsequently removed by sublimation, ultimately resulting in a directional or otherwise tailored porous framework. A simple schematic of the process is illustrated in Fig. 8a. The shape and dimension of ice crystals grown during freezing can be controlled by various factors such as cooling rate, temperature gradient, concentration and composition of solutions, and additional external physical fields. These factors ultimately determine the morphology of the pores and impart distinct physical and mechanical attributes to the structures.[128]

The schematics of several freeze-drying strategies are illustrated in Fig. 8b–g. Conventional unidirectional freezing commences with the suspension being frozen under a single temperature gradient, leading to random ice nucleation on a cold surface. As a result, the solidified suspension media commonly consists of microscale crystallites oriented preferentially along the direction of freezing, resulting in scaffolds with small-scale lamellar pores (Fig. 8b).[129] In bidirectional freezing, ice is allowed to nucleate and grow both vertically and horizontally under dual temperature gradients created by modified freeze-casting configurations, resulting in a large-sized bidirectional aligned porous structure (Fig. 8c).[39] Radial freeze casting is implemented using a copper mold instead of a polymer mold. In this process, the suspension was subjected to two temperature gradients: one along the *Z*-axis of the copper mold and another in the radial direction, resulting in both longitudinally and radially aligned pores (Fig. 8d).[130] Ultrasound-assisted freeze drying is applied to effectively promote the formation of ice crystals during the freezing process because of the pressure and cavitation effects of ultrasound waves.[132] This strategy reduces crystal size and prevents structural damage caused by the overgrowth of ice crystals, leading to a significant decrease in the pore size of porous materials, as shown in Fig. 8e.[131] Additionally, introducing magnetic or electric fields can further control the distribution of suspension media or solid particles in suspensions, resulting in porous structures with various tailored forms.[133,134] However, this technique is infrequently reported in the fabrication of porous polymers due to their poor magnetic and electrical properties.

These porous polymers fabricated by freeze drying have made significant breakthroughs in various fields, including structural biology, thermal insulation, environmental applications, pressure sensors, and energy storage and conversion. Furthermore, the advancement of other innovative methods for building porous structures will continue to drive the utilization of freeze-drying technology in creating biologically inspired structures with enhanced functionality.

3.6. Template method

Template method is a simple but versatile strategy for the preparation of porous polymers.[135–137] Typically, the process involves incorporating sacrificial templates into polymeric solutions or melts. Subsequently, the mixture is solidified through either solvent evaporation or heat removal, after which the sacrificial template is extracted to yield porous structures. A simple schematic of the template method is illustrated in Fig. 9a. In this method, the pore's structures such as size, porosity, shape, and distribution can be effectively regulated by spatial restriction of the templates, ensuring good repeatability and controllability.[138,139] It is evident that the interconnectivity, porosity, and surface area of porous materials increases with the volume fraction of the template. Furthermore, the pore

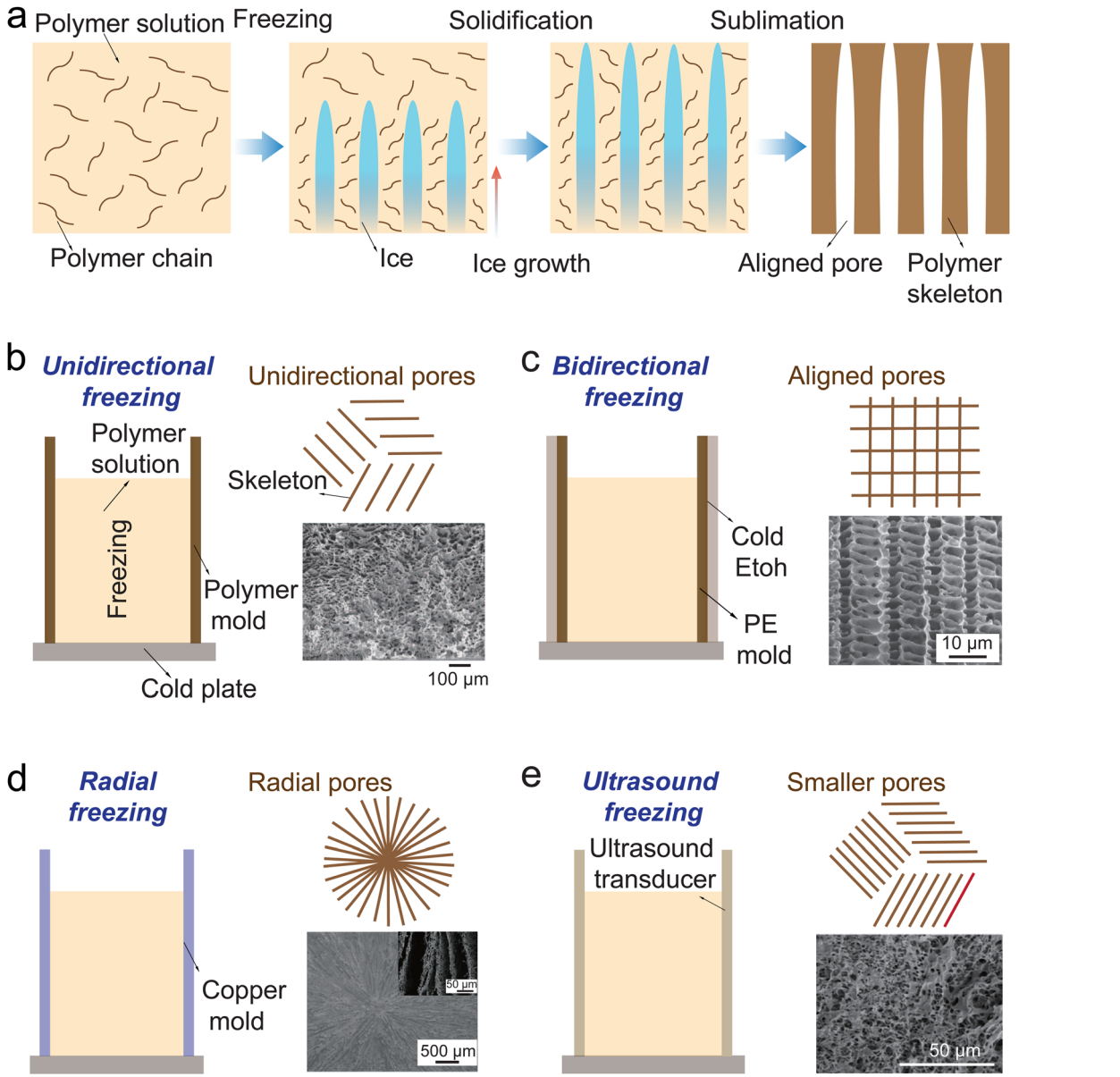

Fig. 8 Freeze drying to fabricate porous polymers. (a) Freeze drying routes of aligned porous polymers. (b)–(e) Schematics of various freeze-drying techniques and top-views of corresponding microstructures of resulting porous polymers: (b) unidirectional freezing (reproduced with permission.[129] Copyright 2015, American Association for the Advancement of Science); (c) bidirectional freezing (reproduced with permission.[39] Copyright 2007, American Ceramic Society); (d) radial freezing (reproduced with permission.[130] Copyright 2019, American Ceramic Society); (e) ultrasound freeze drying (reproduced with permission.[131] Copyright 2023, Society of Plastics Engineers).

structure of porous scaffolds can be manipulated through the shape, weight fraction, and size of the templates.

The template method includes three distinct types: hard-templating, soft-templating, and self-templating. The hard-templating method usually employs rigid or semi-rigid material such as nickel foams, silica, carbon particles, and organic microspheres as physical guides to control pore structures. The operation procedure of this approach is illustrated in Fig. 9b.[140] This method offers almost unrestricted flexibility in the choice of polymer, as long as the target material can either mix with the template or cover its surface. Due to this reason, the hard-templating method offers an emergency and efficient approach to constructing pores within indissolvable polymers. But the method commonly requires multiple steps such as calcination or acid-based etching to remove templates, which might result in pore collapse and destruction. In contrast, the soft-templating method employs soft molecules such as microemulsion droplets, surfactants, or other block copolymers as templates. For example, block copolymers are widely employed for synthesizing mesoporous materials by selective removal of one of the constituent blocks from its precursor (Fig. 9c).[77] In principle, the template can be easily removed by solvents or heating when utilizing microemulsion droplets or micelles as the template. However, it is difficult to achieve

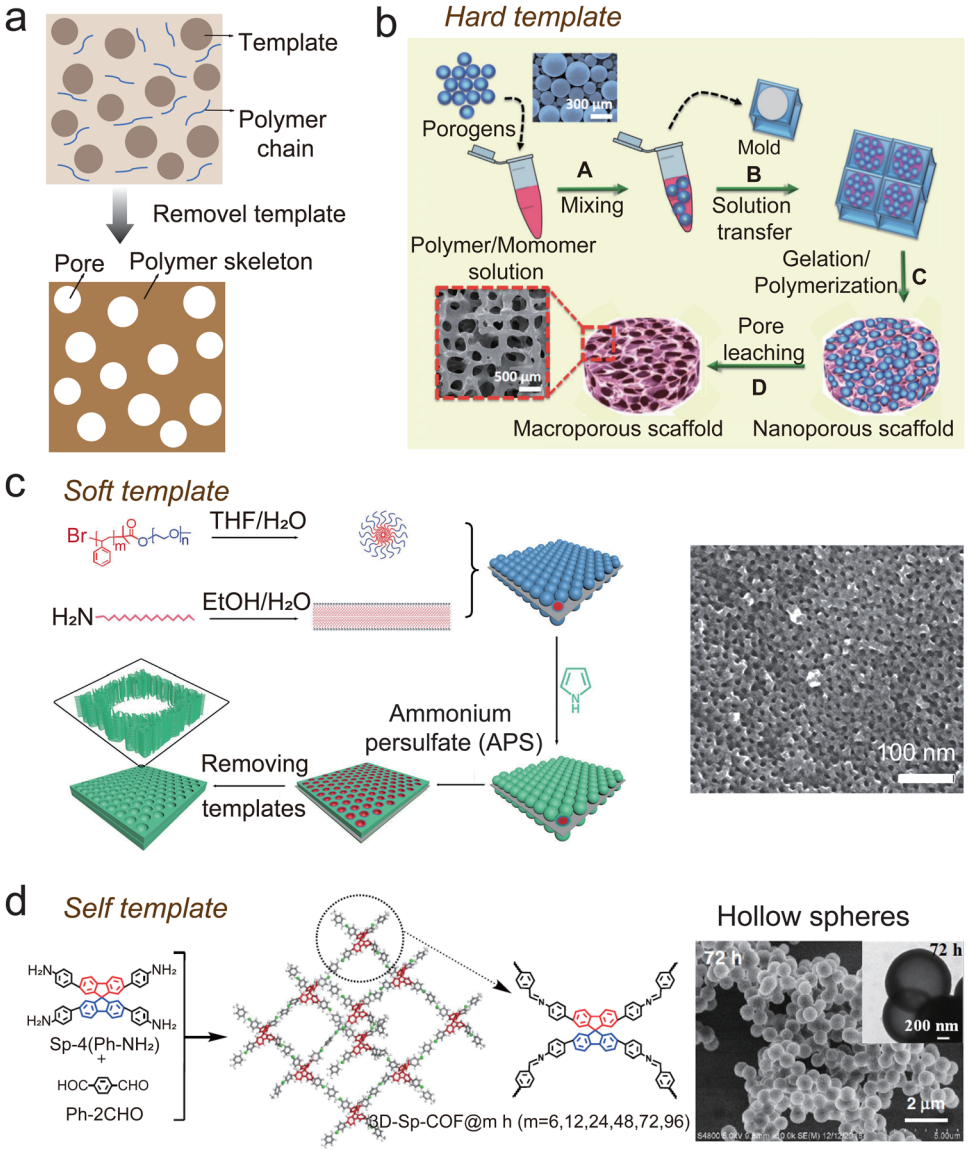

Fig. 9 Template method for fabricating porous polymers. (a) A simple schematic illustration of the sacrificial template method. (b) Illustration of the fabrication steps of a porous scaffold using the sacrificial template. Reproduced with permission.[140] Copyright 2013, Korean Academy of Periodontology. (c) Schematic of the 2D mesoporous polypyrrole (PPy) nanosheets *via* synergic self-assembly of amphiphilic aliphatic amine and PPy-poly(ethylene oxide) block copolymers. Right is the SEM image of the nanosheets, and the scale bar is 100 nm. Reproduced with permission.[77] Copyright 2016, WILEY-VCH. (d) Schematic illustration for the synthesis of 3D-Sp-covalent organic frameworks by self-template method. Reproduced under the terms of the CC-BY Creative Commons Attribution 4.0 International license (**https://creativecommons.org/licenses/by/4.0**).[141] Copyright 2020, The Authors, published by Springer Nature.

precise control for the pore's structure due to the high sensitivity of these soft templates to solvent polarity, pH, and other factors. Self-templating involves a two-step synthesis in which the template materials are fully or partially incorporated into the cores during the fabrication process. The template not only provides support for the porous framework, but also actively participates as a reactant in the formation process of the porous skeleton. It has been widely used for the preparation of hollow polymeric nanospheres, as shown in Fig. 9d.[141] The template is completely or partially consumed during the formation process of the porous skeleton, obviating the post-treatment and rendering it an efficient intracavity pore formation technique. Overall, the template method is straightforward and not harsh, which can synthesize porous polymers with diverse morphologies and structures in a targeted fashion, thus presenting promising prospects for practical applications.

3.7. Comparison of the fabrication techniques for porous polymers

These aforementioned fabricating techniques provide diverse choices to engineer porous polymers with desired porosity, pore size, pore distribution, connectivity, and given functionality. Electrospinning can easily produce porous polymers with high interconnectivity and high porosity, but it has long

Table 1 Comparison of various design techniques for porous polymers

Techniques	Pore formation	Pore geometry	Pore size	Porosity	Connectivity	Production efficiency	Most notable feature	Ref.
Electrospinning	Fibers accumulation	Irregularity; orthogonality; orientation; multistage	Nanoscale to microscale	High	Very high	Low	Easy to obtain nanofibrous membranes	80 91 83 84
Breath figure	Removal of condensed water droplet	Ordered arrays	Microscale	Low	Low	High	High adaptability for curve surface	100 107 108 105
Gas foaming	Bubbles liberation	Relatively uniform spherical pores	Microscale	Very high	High	Very High	No solvents	113 116
Phase separation	Removal of poor polymer phases	Sponge-like; finger-like; gradient pore; porous microspheres	Nanoscale to microscale	Medium	Medium	High	Easy to scale up	123 124 127
Freeze drying	Removal of ice template	Aligned pores; across multiple length-scales	Nanoscale to microscale	High	High	Low	Efficient to fabricate biological structure	128 129 39 131
Template method	Removal of sacrificial templates	Similar in the shape with used template	Nanoscale to microscale	Medium	Low	Medium	Low restriction for materials	135 140 77

Note: some structures and properties may very from case to case.

struggled to improve the material's mechanical strength and production efficiency. BFs are often used to produce ordered pores and are adaptable for curved surfaces, yet accurately predicting the morphology of pores in large-scale production remains challenging. Gas foaming offers the advantage of fabricating high porosity and without requiring organic solvents, but achieving nanoscale pores is difficult due to the growth and fusion of bubbles during the foaming process. Phase separation provides a simple and economical way for producing porous polymers with diverse pore structures, but it involves numerous organic solvents which raises environmental concerns. Freeze drying is particularly effective for creating biomimetic and aligned pore structures. However, it faces challenges in efficiency and industrialization due to limitations in equipment space. In terms of the template method, the main advantage lies in its relatively easy execution without specialized equipment. However, a major drawback is the difficulty in selecting the particle size to achieve high porosity, interconnectivity, and regular pores while maintaining adequate mechanical properties. In addition, 3D printing presents new opportunities for the development of functional porous polymers through its capabilities for geometric manipulation, although this topic is not introduced in detail in this review.[142–144] However, it is not suitable for producing large-scale porous polymers with nanopores because of trade-offs between speed, time, and precision, which often require the combination of sacrificial templates or self-assembly techniques to overcome the challenges. Certainly, it is worth noting that some of the techniques mentioned above may exhibit potential intersections with one another. For example, BFs can also be considered a type of template method because it uses condensed droplets as template; the self-assembly of block copolymers also involves phase separation phenomena between different segments. Nevertheless, we have chosen to discuss them separately in this paper to highlight their respective main characteristics. To clearly illustrate the characteristics of each technique, we present a summary of their fundamental principles of pore formation, pore structures, and other features in Table 1.

4. Applications

The practical properties of porous polymers are closely linked to the pore structure including size, density, connectively, and distribution. Firstly, the construction of a porous structure can significantly reduce the material's elastic modulus and then improve its compression and deformation capability, making it an ideal candidate for use as a highly efficient sensing layer in flexible pressure sensors. Secondly, the existence of pores creates a gas–solid composite structure, resulting in numerous heterogeneous two-phase interfaces within the materials. It has the potential to significantly enhance its ability to reflect and scatter light, sound and other waves, exhibiting fascinating potential in electromagnetic shielding and acoustic absorption. This property is also widely utilized in the thermal

management, including thermal insulation, daytime radiative, and interficial solar evaporator. Thirdly, the channel effect of through pore and the absorption ability from pore walls play key roles in gas/liquid absorption and separation. The size and distribution of pores are crucial parameters that need to be considered in order to enhance the effectiveness of purifying and separating substances across various physical states. Finally, the inherent loading and constraint function of pores can be utilized to incorporate active catalytic groups, electrolytes, tissue cells, or drugs, which are closely associated with the size and connectivity of the pores. Overall, well-defined porous structures are intricately associated with the performance indicators of porous polymers, encompassing elastic modulus, reflection/scattering, channel effect, and space loading and constraint ability. These indicators will ultimately determine the service efficiency of porous polymers as a multifunctional platform in practical applications. In the following section, we will detailed discuss several hot application fields of porous polymers based on the performance indicators influenced by the pore structures. They are flexible pressure sensors, thermal management, electromagnetic shielding, acoustic absorption, gas or liquid adsorption and separation, catalysis, energy storage, tissue engineering, and drug delivery as well as other potential applications.

4.1. Mechanical property

The interior of a porous material is filled with compressible air, leading to significant changes in its mechanical properties. The relationship between elastic modulus (E) and porosity (V_p) for porous materials can be established by introducing a geometrical filling factor (a) that is associated with the spatial organization of the material:[145]

$$E = E_0(1 - aV_p)^{\beta}$$

where E_0 is the initial structural elastic modulus, and β is a constant related to the pore's connectivity and morphology. By the equation, we can see that the construction of a porous structure effectively modifies the material's elastic modulus, as shown in Fig. 10a. Increased porosity results in a lower elastic modulus, improving the compression and deformation capability of materials. This mechanical property of porous materials provides an opportunity for designing high-performance flexible pressure sensors, including piezocapacitive, piezoresistive, piezoelectric, and triboelectric types of sensors that can convert external force stimuli into electrical signal output.[146–149]

For conventional capacitive pressure sensors, the change of capacitance signal is closely related to the variation in thickness ($\Delta d = d - d_0$, d and d_0 represent the thickness of the device before and after deformation, respectively) of the dielectric layer according to the basic electrostatics equation. Furthermore, a new expression can be derived by using easily measurable parameters such as elastic modulus (E) of the dielectric layer and applied stress (σ) to replace d, this can be expressed as:

$$\Delta C = \frac{\varepsilon_r \varepsilon_0 A}{d_0(E/\sigma - 1)}$$

where ε_r, ε_0 is relative dielectric constant and permittivity of vacuum, A is the opposite area of two electrodes. Therefore, porous materials with lower structural stiffness (smaller E) will result in a higher relative change of capacitance (ΔC) under the same external pressure. In addition, porous structure easily achieves elastic deformation, which can suppress the viscoelastic behavior of material and improve the response speed of the device.[153–156] However, low structural stiffness causes a high susceptibility to saturated deformation, narrowing the response range and limiting the sensitivity. Iontronic material provides a new design strategy for developing high-performance pressure sensors. In the iontronic system, capacitance (C_{EDL}) varies in relation to the ion–electron contact area (A_{EDL}) at the EDL interface ($C_{EDL} \propto A_{EDL}$).[157–159] From the Greenwood–Williamson contact theory, A between the rigid object and elastomer can be expressed as:[160]

$$A = \pi N R \int_d^{\infty} (h - d) P_h \, \mathrm{d}h$$

where P_h is the Gaussian height distribution of the rough surface; N is the total amount of hump; R denotes the radius of the hump; h represents the height of the rough surface based on the reference plane. d is the initial distant between the rigid object and elastomer. Furthermore, the moved distance (h–d) of the hump structure during compressive deformation can be denoted as s. Under the same geometry, the N, R, P_h, h and d are constant, and the A positive relates to s which can be expressed as:[161]

$$s = \left(\frac{1}{R}\right)^{1/3} \left(\frac{3P(1 - \nu^2)}{4E}\right)^{2/3}$$

where ν is the passion ratio; P denotes external pressure. Therefore, it can be observed that under constant material and structure, the A between the rigid body and the elastic body during stress deformation is inversely proportional to E, such as $A \propto P/E$. Thus the rate of capacitance change in an iontronic sensor which consists of a smooth electrode layer and rough sensing layer under load, can be expressed as:[162,163] $\Delta C_{EDL}/C_{EDL} \propto \Delta A_{EDL}/A_{EDL0} = \psi P/E$, where ψ is geometrical parameter of the surface topography; A_{EDL0} is the initial contact area between the electrode and dielectric layer; and ΔA_{EDL} is the amount of change in the contact area under the external load. To pursue a larger increment of contact area and higher increment of capacitive, both the initial contact area A_{EDL0} and the E of the sensing layer should be as low as possible. Opportunely, the two requirements can be satisfied simultaneously by increasing the porosity, so that the porous ionic sensing layer is an ideal design for enhancing the sensitivity of pressure sensors. For example, Liu *et al.* proposed a composite porous ionic sensing layer with 95.4% porosity and elastic modulus of only 3.4 kPa, which exhibits both a low initial contact area and high compressibility. The sensitivity of the

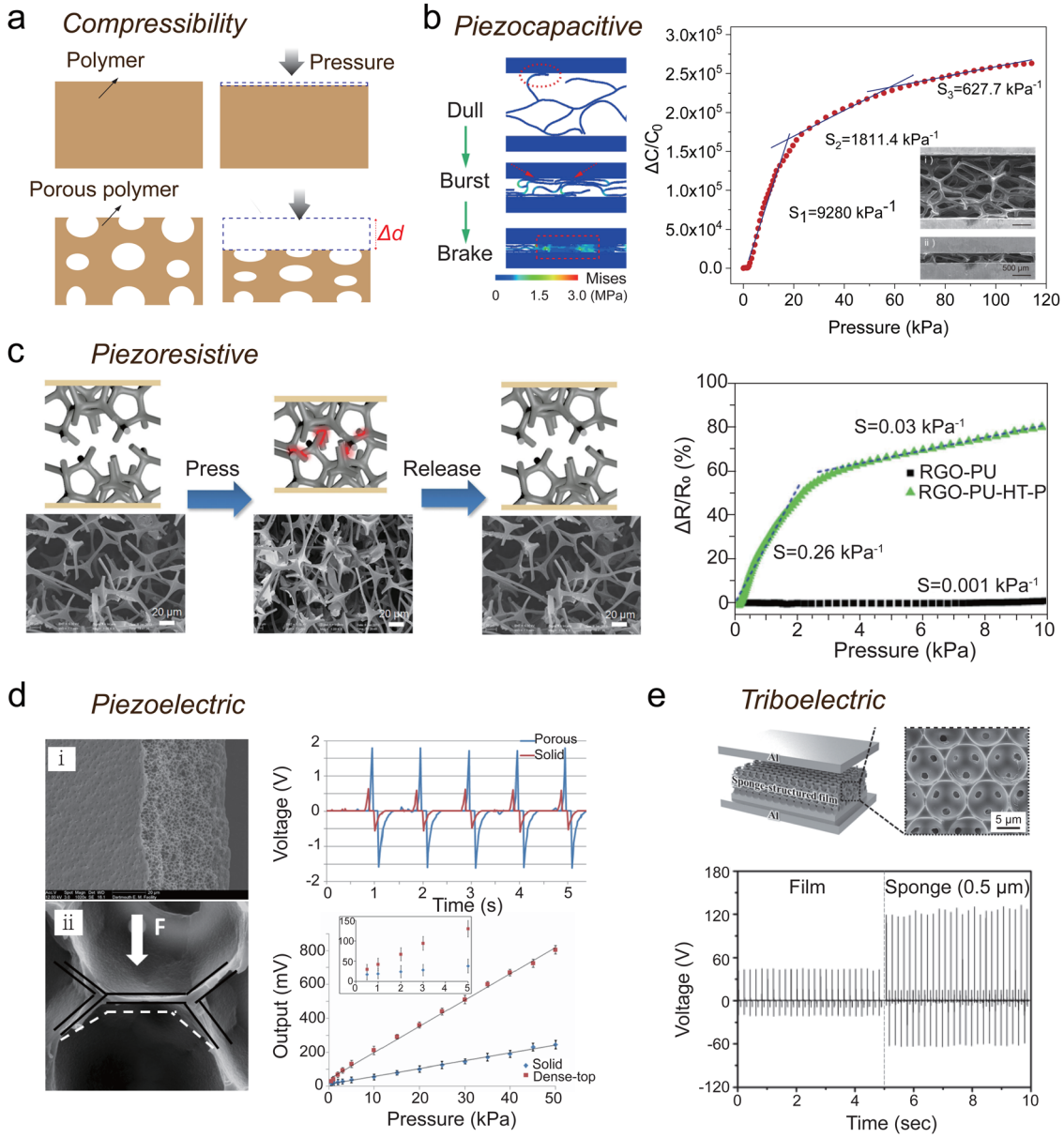

Fig. 10 Porous polymers for flexible pressure sensors. (a) Constructing pores in polymers can effectively reduce the elastic modulus and enhance their sensitivity to external pressure. (b) In the foam-based iontronic capacitive pressure sensors, high-porosity sensing layer brings a low initial contact area and lager compression deformation under the same loading, resulting in a superhigh sensitivity. Reproduced under the terms of the CC-BY Creative Commons Attribution 4.0 International license (https://creativecommons.org/licenses/by/4.0).[30] Copyright 2022, The authors, published by Springer. (c) A reduced graphene oxide polyurethane sponge (RGO-PU) with fractured micropore for piezoresistive pressure sensor. Pressure-dependent change in resistance of the hydrothermally treated and pressed RGO-PU sponge (RGO-PU-HT-P) and RGO-PU sponge, respectively. Reproduced with permission.[150] Copyright 2013, WILEY-VCH. (d) Microporous PVDF membrane for piezoelectric pressure sensing. Output voltage and sensitivities of various sensors based on solid film and porous film under the same pressure. Reproduced with permission.[151] Copyright 2015, IEEE. (e) Porous dielectric layer for improving the performance of triboelectric pressure sensor. Reproduced with permission.[152] Copyright 2014, WILEY-VCH.

porous ionic sensor reaches as high as 9280 kPa^{-1}, setting a new record in the same sensing type at that time, as illustrated in Fig. 10b.[30]

Piezoresistive pressure sensors operate through structural deformation to induce resistance change under external force, thereby converting the pressure signal into resistance or current signal.[164,165] The resistance is defined $R = L/\rho A_R$, where R is resistance, ρ stands for conductivity, L is length and A_R is cross-sectional area. The change rate of resistance can be expressed as $\Delta R/R = (1 + 2\upsilon)\varepsilon + \Delta\rho/\rho$, where υ and ε denote Poisson's ratio and strain, respectively, and $\Delta\rho/\rho$ denotes the resistivity effect. Therefore, the signal variation of piezoresistive sensors is closely related to the change in geometry and conductivity of functional structures. Conventional piezoresistive pressure sensors usually consist of conductive polymers or elastomers filled with conductive particles, which present a low

sensitivity due to limited deformation capability in the functional layer.[166] As mentioned before, constructing pores can effectively decrease the material's compression modulus and improve its strain under external forces, which facilitates the change in resistance and enhances sensing performance.[167] Of course, the rate of change in the contact area between porous skeletons in foam-based sensors remains constrained under compressive stress, resulting in a limited sensitivity. For this reason, Yao *et al.* proposed a design method for a fractured conductive sponge (Fig. 10c), in which the contact area between porous skeleton networks changes instantaneously under external force.[150] This innovative design offers higher sensitivity and enables large-scale production for piezoresistive sensing devices, thus presenting promising prospects for practical applications.

Piezoelectric pressure sensors are passive devices that derive from the potential difference generated by the deformation of piezoelectric material under an external force. Polyvinylidene fluoride (PVDF) is commonly employed as the piezoelectric polymer in these sensors.[168–170] The local micro-mechanical strain of the PVDF porous film can be enhanced by increasing the number and size of pores, resulting in greater deformation and a higher piezoelectric output. Zhang *et al.* optimized the structure of porous PVDF and enhanced the efficiency of electromechanical coupling to improve the piezoelectric effect. The sensitivity of the device reached 16 mV kPa^{-1}, which is three times higher than that of a solid film device at 4.9 mV kPa^{-1}, as shown in Fig. 10d.[151] In addition, triboelectric pressure sensors are another kind of passive devices that utilize the frictional electric effect and the principle of electrostatic induction to convert pressure signals into electrical signals.[171–173] Porous materials exhibit greater change in friction regions under an external force, resulting in an increased power output compared to that of a plain film. For example, Kim *et al.* reported a triboelectric pressure sensor based on a sponge structure, which achieved 130 V output voltage and 0.10 mA cm^{-2} current, respectively. The power output increased by a factor of 10 compared to the solid-type device under the same mechanical conditions, as shown in Fig. 10e.[152]

4.2. Thermal effect

Thermal regulation is a critical characteristic of porous materials, and it has been widely investigated in relevant fields for heat management.[174] Specifically, porous polymers hold great promise for thermal insulation because the pores contain a large amount of air with only 0.026 W m K^{-1} thermal conductivity under the standard.[175,176] Due to the presence of both solid and gas phases, the thermal transmission in porous materials consists of solid conduction (λ_{sol}), gas conduction (λ_{gas}), radiation (λ_{rad}) and convection (λ_{conv}). Total thermal transmission is expressed as the effective thermal conductivity (λ_{eff}): $\lambda_{eff} = \lambda_{sol} + \lambda_{gas} + \lambda_{rad} + \lambda_{conv}$, and a schematic of thermal transmission within a porous material is shown in Fig. 11a.[177] For high-porosity foams or aerogels, the effective thermal conductivity under ambient conditions is primarily determined by gas heat conduction (λ_{gas}), which can be estimated from the equation:[178]

$$\lambda_{gas} = \frac{\lambda_{g0} V_p}{1 + \frac{2\zeta l_m}{D_p}}$$

where λ_{g0} is the thermal conductivity of air, V_p denotes the porosity, $\zeta \approx 2$ for air in aerogels, l_m presents the mean free path of air, D_p is the average diameter of the pores. Therefore, the thermal conductivity of aerogels depends on the porosity, pore size and the mean free path of air molecules (the average distance traveled by gas molecules between collisions). Particularly, the Knudsen effect is particularly observed when the pore size is smaller than the mean free path (<50 nm) of air molecules, leading to inhibited gas conduction. In addition, the solid–gas interface in porous structures can strongly scatter phonons (energy quanta) and the scattering intensity increases with pore size decreases below the mean free range of the phonons, resulting in thermal conductivity even lower than that of air. However, porous polymer are typically used as a thermal controller under relativity mild conditions because polymer easily age at high temperature.

The distribution of pores also significantly influences the material's thermal insulation property. For example, highly aligned anisotropic pores can significantly restrict thermal convection, making them an effective structure for thermal insulation.[179,180] In addition, the pores aligned perpendicular to the thermal gradient increase the density of the solid–gas interface, enhancing the reflectivity of infrared radiation and improving thermal insulation through the multiple reflectance effect at a constant angle of incidence. Kim *et al.* developed an anisotropic waterborne polyurethane (WPU)–boron nitride nanosheets (BNNS) composite porous foam with a low out-of-plane thermal conductivity of 0.0169 W mK^{-1} by using additive manufacturing and freeze-drying. In this composite aerogel, the thermal insulation capability in the transverse direction is significantly superior to that of oriented (Fig. 11b(I)),[78] allowing for a thinner thickness and lighter weight to meet application requirements. The anisotropic pores also play a crucial role in preventing heat loss from the human body. Bai *et al.* produced fibers with oriented porous structures continuously and massively by using freeze-spinning. This bionic fiber is similar to the hollow fiber structure of polar bear hair, presenting excellent thermal insulation properties for thermal stealth, as shown in part II of Fig. 11b.[42]

The mismatched interfaces between the air and solid skeletons within porous polymers result in an inhomogeneous medium that induces significant interface scattering for ultraviolet, visible, and near-infrared light, which can effectively inhibit the thermal effects caused by solar radiation. Although there is typically no direct and quantitative correlation between the thermal radiation emittance of a material and its porosity, smaller pores can further increase the emissivity of thermal radiation. The reason is that the porous structure increases material's surface area and offers more thermal radiation emission sites. As a result, porous polymers have been employed as efficient materials for passive daytime radiative

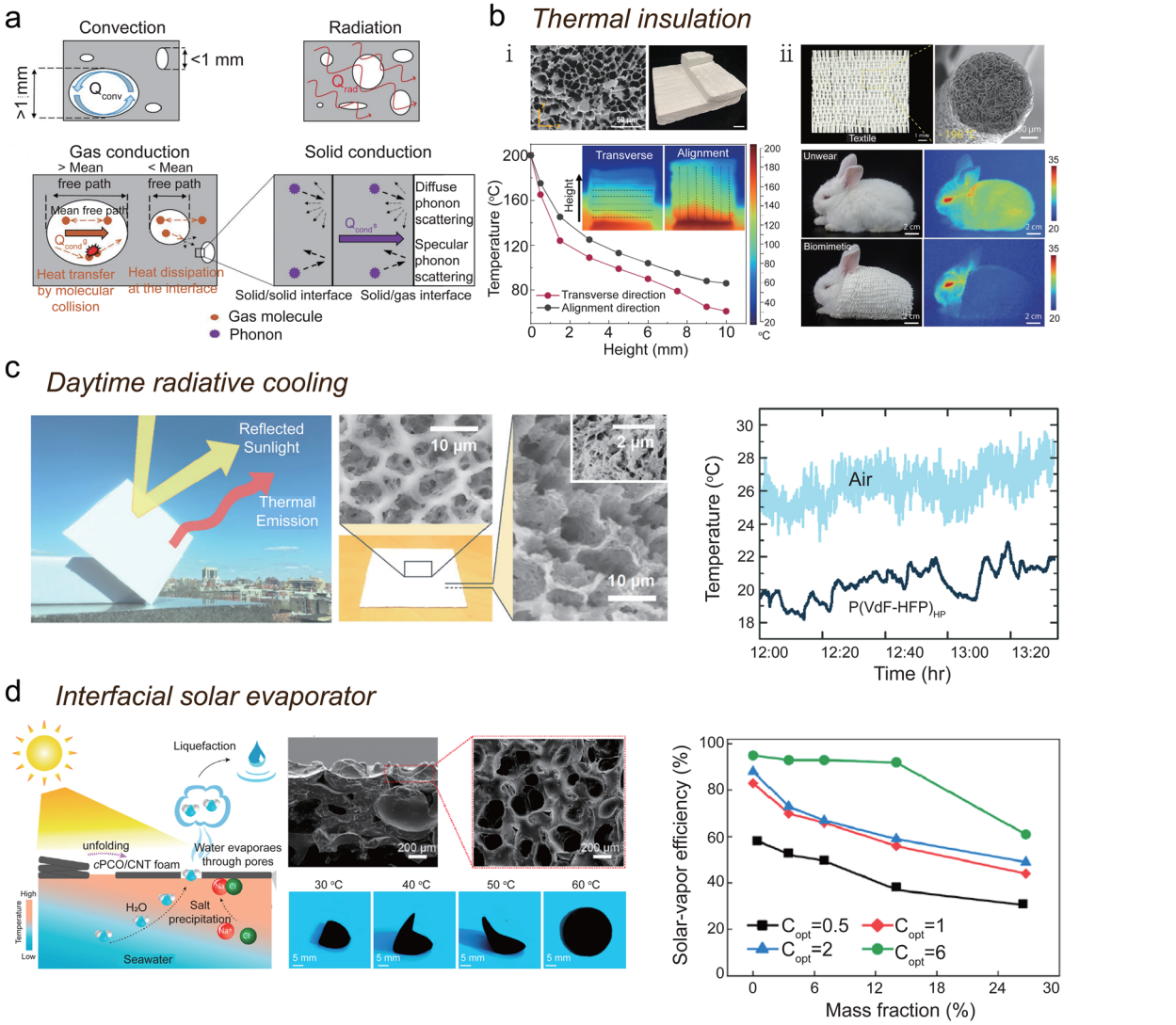

Fig. 11 Porous materials for thermal management. (a) The modes of heat transport in porous materials, involving the convection, radiation, gas conduction, and solid conduction. Reproduced with permission.[177] Copyright 2021, American Chemical Society. (b) Heat-insulation performances of an anisotropic porous aerogel panel (I) (reproduced under the terms of the CC-BY Creative Commons Attribution 4.0 International license (https://creativecommons.org/licenses/by/4.0)).[78] Copyright 2022, The Authors, published by Springer Nature) and a textile from fibers with aligned porous structure (II) (reproduced with permission.[42] Copyright 2018, WILEY-VCH). (c) A hierarchically porous PVDF-HFP for highly efficient passive daytime radiative cooling. Reproduced with permission.[43] Copyright 2018, American Association for the Advancement of Science. (d) A shape programmable solar evaporator with porous foam, and its morphology and solar-to-vapor conversion efficiency. Reproduced with permission.[44] Copyright 2021, American Chemical Society.

cooling.[181–184] The radiative cooling model exhibits strong thermal energy emission and minimal sunlight absorption, without requiring electricity, refrigerants, or mechanical pumps. Y. Yang and N. Yu utilized a phase separation technique to prepare a multiscale porous polyvinylidene fluoride-hexafluoropropylene (PVDF-HFP) coating, which demonstrated 95% solar reflectance and 98% infrared transmittance. This resulted in an impressive cooling performance of about 6 °C under a solar insolation of 890 W m^{-2} and an ambient temperature of 26.5 °C (Fig. 11c).[43] Furthermore, porous polymers and their composite materials have great potential for solar-driven water evaporation.[185–187] These water evaporators demonstrate several advantages such as broad absorption of sunlight, low thermal conductivity, open pores facilitating rapid water molecule transport, and high energy conversion efficiency. The properties of porous materials can effectively absorb sunlight at the water/air interface and convert it into heat, achieving localized and precise high temperatures while dramatically increasing the evaporation rate of water. This approach offers a feasible solution to address the limitations of energy transfer and loss in traditional water evaporation heating modes. Zhao *et al.* designed a flexible solar evaporator with high efficiency, foldability, and monitoring of salt clogging by using shape memory porous composites (Fig. 11d). The

device achieved an energy transfer efficiency of 83% and a steam production of 1.26 kg m^{-2} h at one sun, it is comparable to advanced solar evaporators.[44]

4.3. Wave regulation

The pores in porous materials produce numerous spaces and air/polymer interfaces, which can act as an effective shielding or absorbing materials for impeding the transmission of diverse waves, including electromagnetic wave and acoustic wave. For electromagnetic interference (EMI) shielding,the total shielding efficiency (SE_T) of materials can be expressed as follows:[188,189] $SE_T = 50 + 10\log(\sigma/f) + 1.7d\sqrt{\sigma f}$, where f is the frequency of incident EM waves, d is thickness of material, and σ denotes electrical conductivity. Therefore, the EMI shielding performance shows a robust positive correlation with the σ and d of the shielding material, indicating that materials with high electrical conductivity are necessary for EMI shielding. However, considering the skinning depth $\delta = (1/\pi f\ \mu\sigma)^{1/2}$ where μ represents permeability,[190] it is noted that high electron mobility will result in a reduced skin depth for electromagnetic wave radiation. This means that a majority of the electromagnetic waves are reflected on the material's surface rather than penetrating its interior, causing secondary electromagnetic pollution. Porous conductors not only improve the impedance matching at the air shielding interface by influencing the surface conductivity of air shielding but also enhance multiple reflection and scattering attenuation of electromagnetic waves due to abundant internal mismatch interfaces (Fig. 12a), making them an optimal choice for EMI shielding.[191–193] Nevertheless, conventional polymers have poor electrical conductivity and therefore require compounded with carbon-based materials, metals, MXene, or other conductive fillers to enhance electrical conductivity. It can help to contribute to stronger conductive loss and more considerable polarization loss.[194–197] For example, Cheng *et al.* developed a lightweight and flexible graphene-PDMS foam with a high electromagnetic shielding effectiveness of 44.7 dB at a film thickness of approximately 1.2 μm as shown in Fig. 12b.[41] The porous filler/polymer composite materials can achieve desirable properties such as low density, good processability, adjustable conductivity, and structural stability. Consequently, they represent a promising option for a lightweight electromagnetic interference shielding system, effectively overcoming the limitations associated with conventional metal materials such as high weight, poor corrosion resistance, and secondary electromagnetic wave contamination.[198]

Furthermore, open pores offer natural channels that allow sound waves to penetrate deeply into materials. Once the sound waves propagate through these pores, the sound energy will be dissipated due to thermal effects from frictional resistance of air with pore walls, viscous resistance of air, and skeleton damping,[199] as illustrated in Fig. 12c. However, the dissipation force is a linear function of the rate, and the dissipation power is the product of the force and the flow rate. As a result, sound dissipation power (P_d) is a quadratic function of the frequency ($P_d \propto f^2$). As a result, conventional porous polymers such as foams and fibers exhibit inherent inefficiency for absorbing or attenuating low frequency sound.[200–202] Increasing the specific surface area or thickness of porous polymers can enhance the dissipation power for sound waves, but it will result in a significant increase in the material's weight, which is insufficient to meet the increased demands for acoustic protection of industrial machinery, household appliances, vehicles, and buildings. To enhance the acoustic absorption efficiency of porous polymers, an effective approach is to design gradient pores capable of altering the degree of spatial curvature. This structure can enhance multistage reflection and dissipation of incident soundwaves at the air/polymer interface, causing multiple reflections and friction to dissipate more energy. Ding *et al.* reported a gradient fibrous sponge with fluffy/semi-fluffy/dense by multijet blend electrospinning. This porous material exhibited exceptional broadband sound absorption, achieving a noise reduction coefficient of up to 0.53 (see Fig. 12d).[40] However, the sound absorption frequency of materials relying only on porous structure is primarily in the mid and high frequencies, and there is a need to improve their ability to absorb low-frequency sound waves. Porous piezoelectric materials have the capability to produce an electrical potential or voltage that is directly proportional to force, making them valuable for converting mechanical energy into electric potential and heat for acoustic control.[203] In addition, ultrathin graphene sheets present rich vibrational characteristics due to large out-of-plane deformation under mechanical actuation, providing an ideal candidate for fabricating high-efficiency acoustic absorbers when combined with porous polymers.[204]

4.4. Channel and absorption effect

Porous polymers with well-defined pores and surface chemistry provide efficient channels for high-speed fluid transport (Fig. 13a), attracting significant attention in the field of gas/liquid filtration and separation. For example, air filters composed of polymeric fibers can be employed for the filtration of particulate pollutants such as $PM_{2.5}$.[205,206] The filtration performance is evaluated by filtration efficiency (F_e) and pressure drop (ΔP), which can be respectively expressed as:[207]

$$F_e = 1 - \exp\left[\frac{-4\alpha\eta Z}{d_f\pi(1-\alpha)}\right]$$

$$\Delta P = 64\mu U_0 \frac{\alpha^{3/2}(1+56\alpha^3)}{d_f^2} Z$$

where η is the filtration efficiency of a single fiber, α denotes the fiber volume fraction, Z is the thickness of the filter, d_f is the average diameter of the fiber, μ represents the air viscosity, and U_0 is the surface velocity through the air filter. The above model indicates that increasing filter thickness and decreasing fiber diameter can enhance the filtration efficiency of porous filters. However, thicker filters with a dense build-up of finer fibers will affect the circulation of airflow and then cause high resistance, resulting in a challenge in balancing air pressure drop and filtration efficiency. When fiber's diameter approaches the

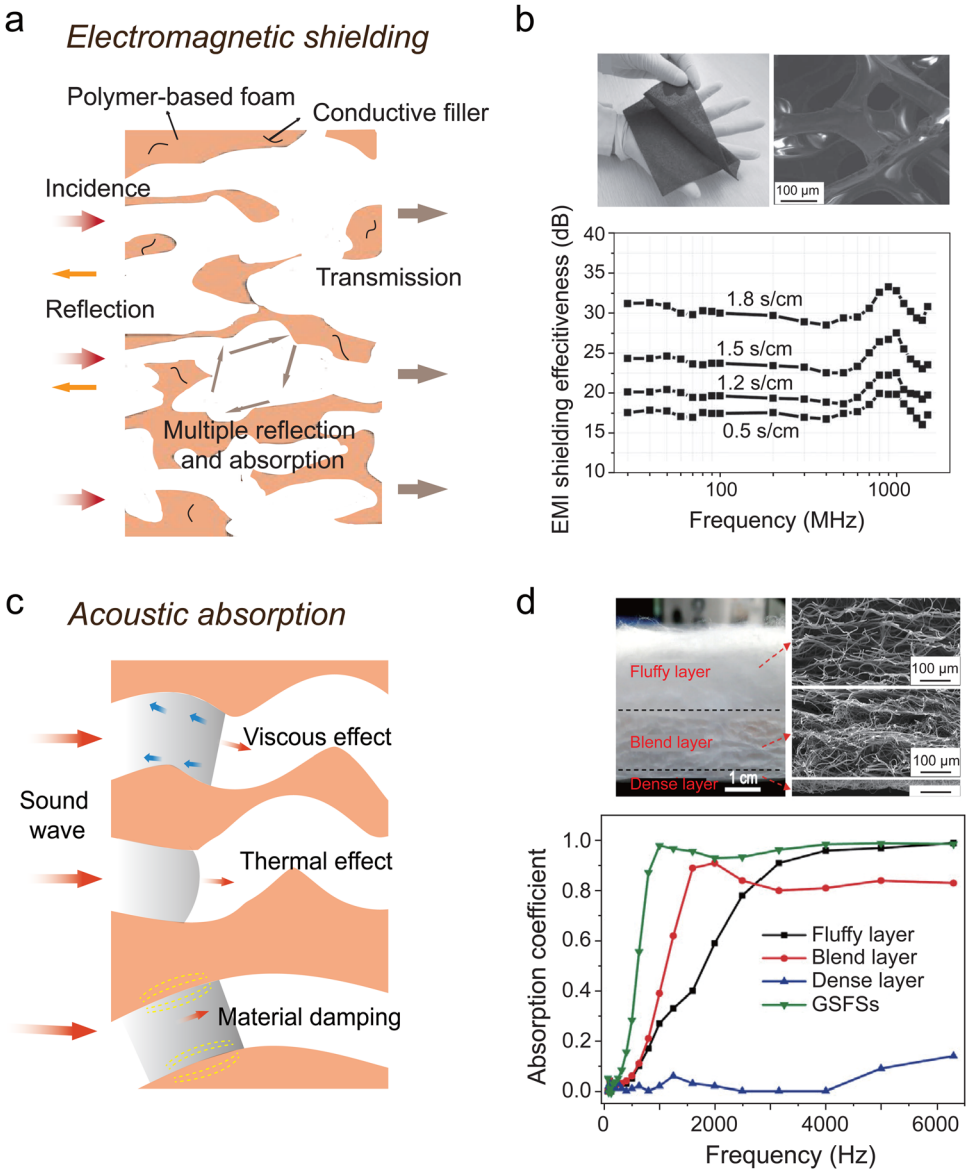

Fig. 12 The porous polymers regulate electromagnetic and acoustic waves. (a) The mechanism of EMI shielding of porous materials. (b) The EMI shielding effectiveness of a graphene/PDMS composite foam. Reproduced with permission.[41] Copyright 2013, WILEY-VCH. (c) Schematic diagram of the energy consumption mechanisms of porous materials. (d) Gradient porous fibers serve as broadband sound absorption. Reproduced with permission.[40] Copyright 2021, Elsevier.

mean free path of air molecules (66 nm under standard conditions) and its surface chemistry matches that of the particulate pollutants, nanofibers present a low airflow resistance and high PM capture efficiency simultaneously due to the 'slip' effect and stronger intermolecular forces. This enables a balance between high efficiency and low resistance, making it possible to achieve optimal filtration performance.[208] Cui *et al.* have reported a series of innovative works in porous air filters. They utilized electrospinning to fabricate porous polyacrylonitrile (PAN) nanofibrous with ultra-fine diameters and specific surface chemistry for air filters. The porous membranes exhibit the capability of removing 96.12% $PM_{2.5}$ at a pressure drop of 133 Pa (Fig. 13b),[49] and hold potential for applications in innovative masks, indoor environmental protection, and other related fields. In addition, highly porous membranes, in which microporous structures serve as high-speed gas transport channels, have advanced the field of gas separation.[209] Nevertheless, fabricating ultrathin and large-area microporous membranes is a challenge due to the inherent difficulties in eliminating defects.

For the separation and purification of liquids, porous polymer membranes also offer many promising advantages such as high durability and the absence of phase change during the separation process.[211,212] However, microfiltration and ultrafiltration membranes present high permeation flux and filtration efficiency for macromolecules, but they are inadequate for the

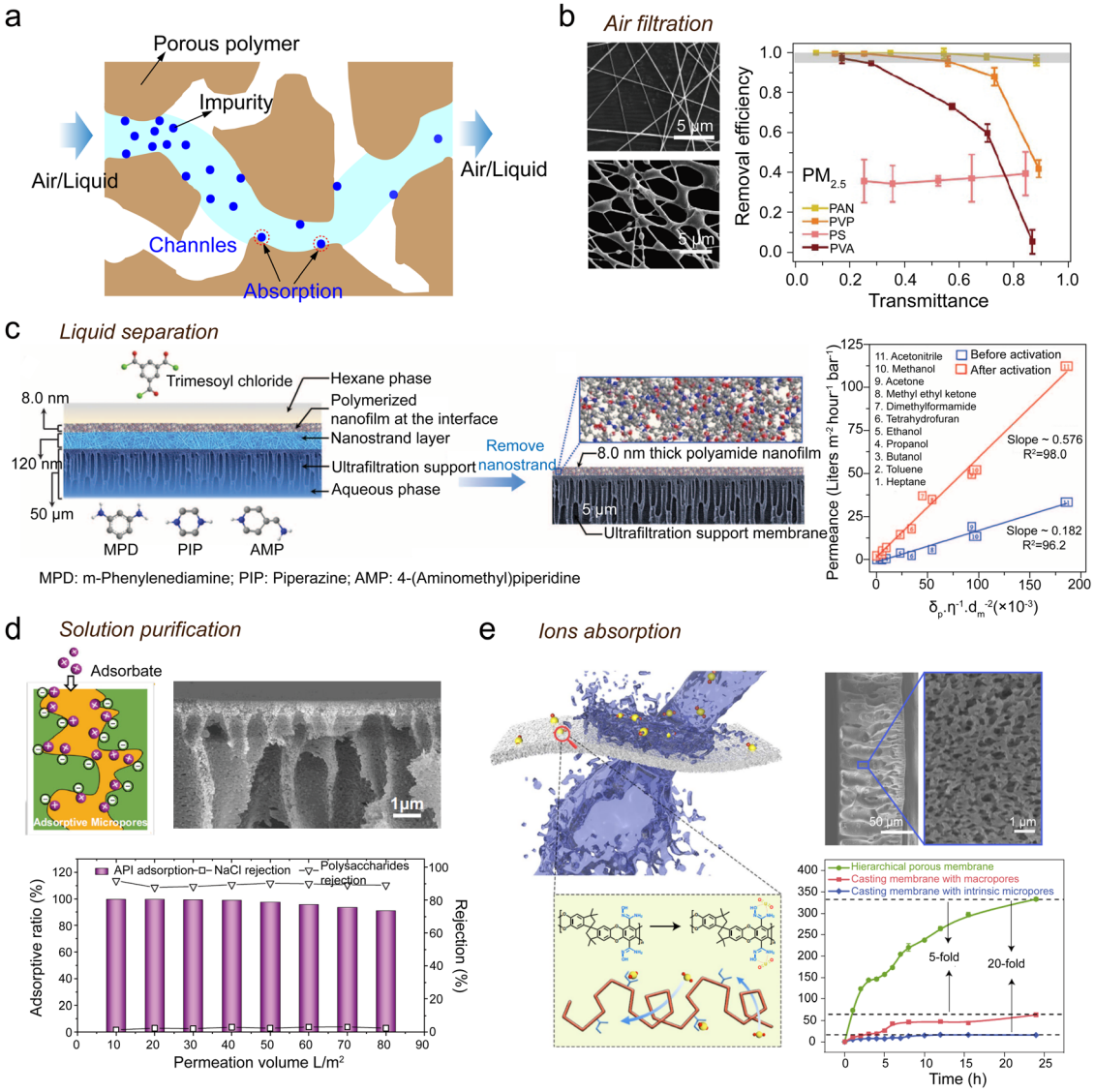

Fig. 13 Adsorption and separation capabilities of porous polymers. (a) The schematic of the channel and absorption effect of porous polymer. (b) A porous fiber filter for high-efficiency $PM_{2.5}$ capture. Reproduced with permission.[49] Copyright 2015, Macmillan Publishers Limited. (c) A composite porous membrane with gradient pore size for ultrafast solvent transportation and molecular separation. Reproduced with permission.[50] Copyright 2015, American Association for the Advancement of Science. (d) A porous hydrophilic amidoxime modified adsorption membrane to selectively adsorb and separate small organic molecules from water. Reproduced under the terms of the CC-BY Creative Commons Attribution 4.0 International license (https://creativecommons.org/licenses/by/4.0).[210] Copyright 2022, The Authors, published by Springer Nature. (e) Hierarchical porous membrane for efficient uranium extraction from seawater. Reproduced under the terms of the CC-BY Creative Commons Attribution 4.0 International license (https://creativecommons.org/licenses/by/4.0).[51] Copyright 2021, The Authors, published by Springer Nature.

separation of nanoscale organic molecules. The filtration of organic molecules requires nanoscale pores and selective membranes, but smaller pores inevitably lead to decreased solvent permeation flux according to Kozeny–Carman equation (see Section 2). To address this challenge, Livingston *et al.* proposed a multilayer porous structure that forms an approximately 10 nm thick polyamide (PI) as a separation layer by interfacial polymerization on the surface of a porous ultrafiltration membrane. This composite porous structure provided high solute retention under pressure filtration, achieving an acetonitrile permeation rate of up to 112 liters m^{-2} $hour^{-1}$ bar^{-1}, as shown in Fig. 13c.[50] Furthermore, to improve the purification efficiency of the solution, the researchers proposed a dynamic adsorption technique that exploits specific membrane-solute interactions including electrostatic interactions, π–π interactions, van der Waals forces, and hydrogen bonding, achieving highly selective and rapid separation of organic molecules. Traditional polymer membranes have a limited specific surface area and adsorption sites, restricting their ability to handle low-concentration solutions. Enriching the adsorption sites of porous polymers through functional modification is an effective strategy to improve adsorption efficiency. For example,

Wang *et al.* modified polymers by using kainimine oxime to improve their solution processability while providing richer adsorption sites, resulting in a 99.9% removal rate for organic molecules and a permeation flux two orders of magnitude higher than that of a conventional nanofiltration membrane (Fig. 13d).[210] Furthermore, Wen *et al.* have also developed a bionic hierarchical porous adsorption membrane based on intrinsic microporous polymers. The structure with decreasing pore size allows uranyl ions to rapidly diffuse into the membrane and then fully exploit the abundant adsorption sites in the micropores, improving the adsorption capacity to 20 times that of the initial membrane (Fig. 13e).[51]

4.5. Spatial loading

Pores in solid bulks, like many microvessels, provide abundant storing spaces for active substances such as catalysts, electrolytes, tissue cells and drugs (Fig. 14a). This plain nature of porous materials aroused the interest of scientists, who have already carried out a great number of attempts in catalysis, energy storage, tissue engineering, and drug release. The porous polymers with high porosity, large surface area, and open channels are attractive hosts for heterogeneous catalysis.[213–216] The incorporation of essential catalytic sites into porous frameworks is a universal approach for obtaining porous catalysts.[217] The porous polymer-based catalysts have the potential for high catalytic activity and selectivity, superior stability, simple recovery, and easy recycling. Thomas *et al.* introduced bipyridine moieties into the backbone of covalent organic frameworks (COF), enabling the coordination of Co^{2+} within the hierarchical pore structure (macro-TpBpy-Co). This material exhibits a competitive overpotential of 380 mV at 10 mA cm^{-2}, presenting a significantly enhanced OER activity compared to purely TpBpy-Co (Fig. 14b).[45] Moreover, the further functionalization of porous polymers and fillers can significantly improve their energy storage performance in terms of capacity, energy density, lifespan, and stability.[218–220] Cui *et al.* reported a safe solid polymer electrolyte, which employed an ultrathin nanoporous PI film to load polyethylene oxide/lithium bis(trifluoromethane sulfonyl)imide (PEO/LiTFSI). The vertical channels enhance the ionic conductivity (2.3×10^{-4} S cm^{-1} at 30 °C) of the loaded polymer electrolyte. Meanwhile, the lithium–ion batteries fabricated with PI/PEO/LiTFSI solid electrolyte show high cycling performance at 60 °C and are able to withstand abuse tests such as bending, cutting, and nail penetration (Fig. 14c).[47]

Degradable porous polymers are a favorable option to load the biological cells or molecules for the regeneration of new tissues, known as the tissue engineering technique. This approach requires that porous scaffolds can balance temporary mechanical function with mass transport to aid biological delivery and tissue regeneration.[221–223] Generally, more than 90% porosity, highly interconnected pores, as well as micrometer even millimeter-scale pore diameter are necessary for cell penetration and growth. Ma *et al.* developed a porous scaffold capable of controlled release of recombinant human bone morphogenetic protein-7 (rhBMP-7) to enhance bone regeneration (Fig. 14d).[46] In addition, porous nanomaterials can as carriers to encapsulate or load therapeutic agents and deliver them to the intended targets, known as drug release.[224,225] Obviously, drug leaching is difficult to prevent in surface loading, whereas it can be minimized when the drug is encapsulated in pore channels. Therefore, utilizing porous carriers for encapsulating poorly soluble and unstable drugs not only increases the efficiency of existing medications but also well overcomes many challenges faced by other nanocarriers, such as drug uptake capability and controlled release.[226,227] Feng *et al.* introduced a microporous polymer that functions as an integrated platform for light-induced programmable drug delivery in cell-based assays (Fig. 14e).[48] By employing light irradiation, the cyclodextrin-azobenzene host–guest complexes formed on the polymer can undergo from an ''associated'' to a ''dissociated'' state, providing precise photochemical control over the supramolecular coding system and its surface patterning ability.

4.6. Correlation between the applications, pore structures and fabrication techniques of the porous polymers

The introduction to the various applications of porous polymers illustrates that the pore structure confers a lower compression modulus, enhances mass transfer efficiency, improves spatial loading capability, and changes the interface interaction between the material and environment, thus significantly improving its applicability. Table 2 presents a summary of the correlation between the application of porous polymers, pore structures and fabrication techniques. The compressibility deformability of sensing layer is primary focus to improve the sensitivity of a flexible pressure sensor, which is determined by the porosity of the sensing layer. High porosity can induce a lower elastic modulus and effectively increase the deformability of porous polymers, and this structure can be easily achieved by gas foaming. In thermal management, the space constraint and interface scattering/reflection effects from anisotropic and microscale pores are the key factors for performance improvement. In addition, the channel effect of pore structure also is an attractive in interfacial solar evaporator to help transmission steam. Electromagnetic shielding and acoustic absorption mainly apply the absorption and reflection effect of porous polymers. The pore structures, characterized by high porosity, open pores, and a high specific surface area, are highly favorable for enhancing the absorption and reflection capabilities of porous polymers, which can be fabricated through freeze drying, electrospinning, gas foaming and phase separation. In addition, the adsorption and separation of gases or liquids make use of the channel and adsorption effects from porous polymers. It is worth note that the presence of through and hierarchical pores obtained by phase separation technique is essential for liquid separation, solution purification and ions absorption in order to achieve high permeation flux and filtration/absorption efficiency. The other applications, such as catalysis, energy storage, tissue engineering scaffold, and drug release, all concern the spatial load ability of porous polymers.

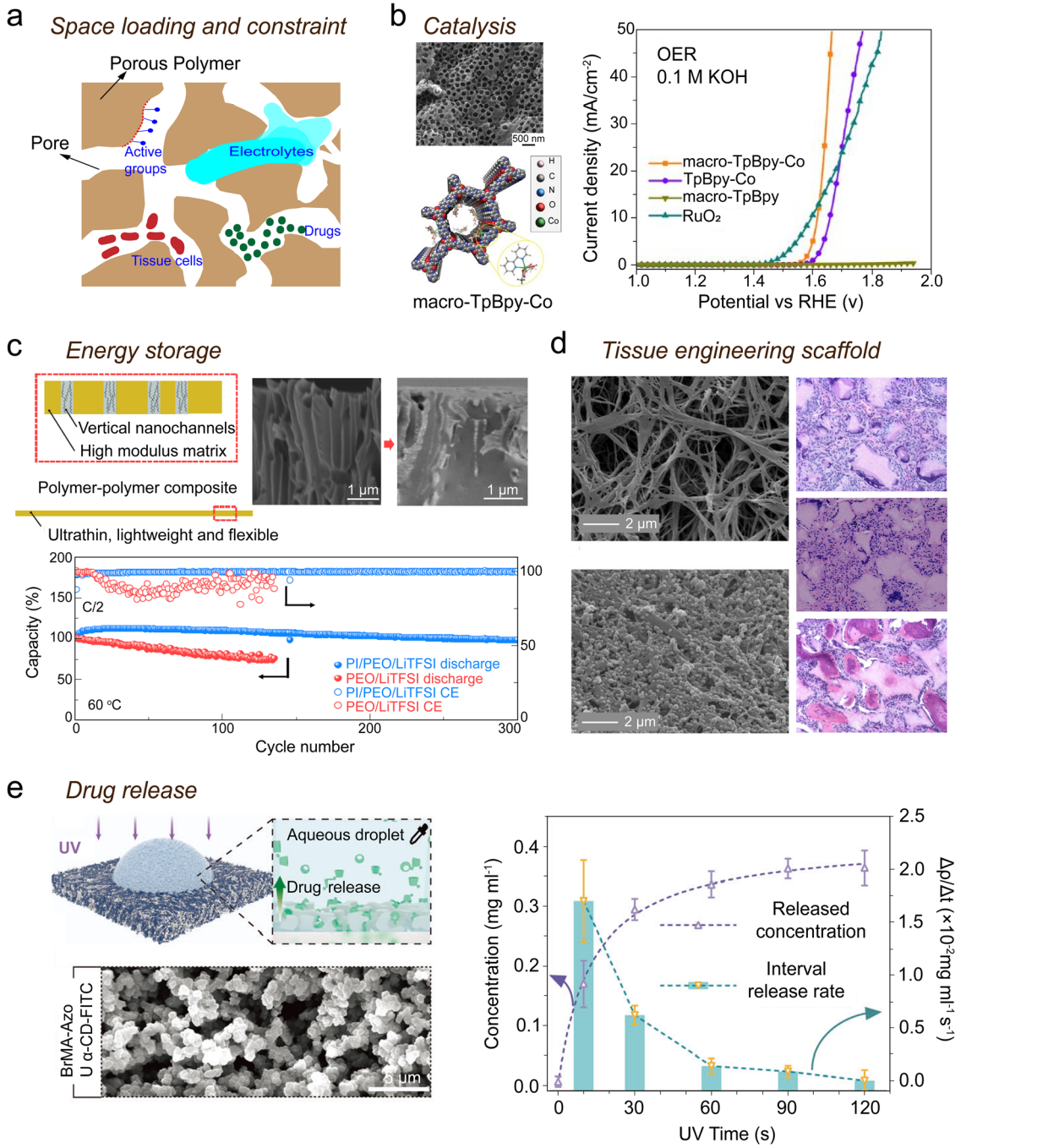

Fig. 14 The porous polymers applied in catalysis, energy storage, tissue engineering scaffold, and drug release. (a) The schematic of the space loading and constraint capacity of porous polymers. (b) A conjugated microporous polymer for heterogeneous catalysis. Reproduced with permission.[45] Copyright 2019, American Chemical Society. (c) A solid-state electrolyte with an 8.6-μm-thick nanopore PI film filled with PEO/LiTFSI serves as a safe solid polymer electrolyte. Reproduced with permission.[47] Copyright 2019, The Authors, published by Springer Nature. (d) A porous nanofibrous incorporating rhBMP-7 nanospheres for osteogenesis. Reproduced with permission.[46] Copyright 2007, Elsevier. (e) A microporous polymer is developed for light-induced programmable drug release in cell-based screening. Reproduced with permission.[48] Copyright 2023, Wiley-VCH.

Open pores are a fundamental requirement for these applications as it is necessary to ensure seamless interaction between the loaded active materials and the external environment. Certainly, we have just discussed the part applications of porous polymers and their desired structure, as well as the corresponding fabrication techniques reported in the literature. In actual production, greater emphasis is placed on balancing product efficiency with production cost. It is therefore that the systematic understanding of the material structure required for each application field, as well as the

Table 2 Summary of the relevancy between the applications of porous polymers and their pore structures and fabrication techniques

Applications	Types	Utilized functions of porous polymers	Desired pore structures	Fabrication techniques	Ref.
Flexible pressure sensor	Piezocapacitive Piezoresistive Piezoelectric Triboelectric	Compressibility deformability	High porosity	Gas foaming Phase separation Template method	30 150 151 152
Thermal management	Thermal insulation	Space constraint and reflection effects	Anisotropic pore	Freeze drying	177 78
	Daytime radiative cooling	Emissivity and interface scattering	Microscale pore	Phase separation	43
	Interfacial solar evaporator	Space constraint and channel effects	Through pore	Template method	44
Electromagnetic shielding	—	Absorption and reflection effect	High porosity; open pore; high specific surface	Freeze drying; Electrospinning; Gas foaming	196 197 198
Acoustic absorption	—			Electrospinning; phase separation	40
Adsorption and separation	Air filtration	Channel and adsorption effect	High porosity; through pore; high specific surface	Electrospinning	49
	Liquid separation Solution purification Ions absorption		Through pore; hierarchical pore	Phase separation	50 210 51
Others	Catalysis Energy storage Tissue engineering scaffold Drug release	Spatial load effect	High porosity; open pore Through pore; Open pore; large pore; Open pore; nanoscale pore	Gas foaming Phase separation Electrospinning Phase separation	45 47 46 48

characteristics of the preparation means of these structures, can provide more valuable solutions for actual design and production of produces.

5. Conclusion and prospect

This review comprehensively introduces the fundamental structures, fabrication techniques, and various existing applications of porous polymers, assisting readers in quickly familiarizing themselves with the available design ideas within this research field. Among these, the morphology of materials mainly involves the pores and solid skeleton, which jointly determine the material's performance. In terms of the pore structures, the traditional division of the pore size is mainly on a nanoscale. However, in future considerations, pores with larger sizes (microns or even millimeters) should be included. The other parameters, such as porosity, pore connectivity, and distribution, are also introduced in detail from their basic principles and applicable scenes. In addition, the surface chemistry is determined through careful selection of the raw materials or loading extra functional fillers. This paper does not give an in-depth introduction to this aspect, as it has been extensively reviewed in other literatures. In fact, it is often necessary to have multiple suitable parameters simultaneously in pores to achieve a specific functional material. As such, the coordination of several structural parameters should be thoroughly explored and systematically analyzed in the future, which will offer more high-quality options for structural design in functional materials. Of course, achieving high-performance and desirable materials solely through pore structure adjustment is generally challenging. It often requires enhancing the functionality of porous materials through composite or surface treatment techniques.

In terms of fabrication techniques, each technique presents unique advantages for the customization of porous polymers with well-defined pore structures. (1) Electrospinning produces porous materials through stacking nanofibers, enabling the creation of regular, layered, and biomimetic structures with high porosity and through pores. Nevertheless, it encounters challenges in terms of mechanical properties and production efficiency. The advancement of materials, as well as multi-needle and needleless methods, are expected to address these dilemmas in the electrospinning technique. (2) The BFs method is a promising technique for fabricating ordered pores even on a curved surface. However, one obvious limitation is that the adopted polymer needs to dissolve in highly volatile organic solvents, resulting in a limited material selection. (3) Gas foaming has advanced to become a commercially successful production technique. It exhibits a great advantage for fabricating porous foams with high porosity and mechanical strength. The potential for meaningful exploration in the future lies in developing strategies for achieving nanoscale pores using this technique. We believe that directly reconstructing

the microscale pores in an initial foam may be a feasible and effective approach to achieving this goal. (4) Phase separation does not necessitate costly and specific equipment, and it can obtain abundant pore structures by adjusting solution concentration, solvent and non-solvent systems, or cooling rate. Although the size and distribution of the pores are difficult to maintain high homogeneity by phase separation technique, we think that the method is still an ideal way for producing porous polymers to meet industrial demands due to its diverse forms and economical production. (5) Freeze casting can be utilized to fabricate well-defined anisotropic pores by controlling the direction and speed of ice crystal growth. In the future, it is anticipated that integrating freeze casting with other manufacturing techniques (such as 3D printing or electrospinning) to generate serviceable biomimetic porous polymers. (6) Template methods allow the control of the size, morphology, and arrangement of porous polymers through the spatial confinement effect of template agents, providing reproducibility and controllability for pore structure. We recommend that researchers prioritize this method for fabricating porous polymers due to its simplicity, especially the hard template method. Overall, whether the pore size ranges from nanoscale to microscale, low porosity with closed pores to high porosity up to 99% with all-through pores, or highly regular distribution to multilevel gradient structure, almost can find one or more appropriate fabrication techniques introduced in this review to achieve these wanted structures. Certainly, considerable advancements have been achieved in the preparation techniques of porous polymers, but no singular technique reigns supreme. The optimal approach is to select a suitable technique for producing porous polymers or their composite materials tailored to specific application requirements. Furthermore, it is essential to fully consider a combination of multiple techniques in order to achieve personalized pore structure at various scales while maintaining sufficient framework stability. However, the real challenge lies in how to obtain composite structures such as both nanoscale pores and high porosity, both high connectivity pores and high mechanical strength, and so forth. Another hurdle is how to exploit a simple and efficient technique to precisely control the pore's distribution in polymeric bulk, allowing for free design. Additionally, the utilization of cost-effective raw materials, programmed production, and acceptable performances are crucial factors for the advancement of industrial applications in the future.

Constructing pores can effectively enhance polymer's properties in mechanical, thermal, optical, electrical, and magnetic aspects, enabling wide applications in the fields of flexible sensing, thermal management, electromagnetic shielding, acoustic absorption, adsorption, and separation. Specifically, pore structures can significantly reduce the material's elastic modulus, providing an opportunity for flexible pressure sensors to enhance their sensitivity. However, different applications require specific sensing properties beyond just sensitivity under applied load. Therefore, further understanding the relationship between the porous structure and the other sensing performances such as hysteresis, response speed, and stability is essential. In addition, a large number of pores and air/skeleton interfaces in porous structures play a crucial role in restraining the propagation of light waves, sound waves and electromagnetic waves, presenting important research value in terms of thermal control, electromagnetic shielding, and acoustic reduction. Among these, enhancing the chemical and physical stability of porous polymers is a critical focus in thermal management and necessitates meticulous engineering. In the fields of electromagnetic shielding and acoustic reduction, the pursuit of devices that are ultrathin and highly efficient is a constant endeavor. The exploration of impressive absorbing structures inspired by nature and understanding their principles is anticipated to offer novel insights for the development of the next generation of ultra-thin absorbers. While porous polymers have well-established applications in ion exchange, adsorbent resins, and polymeric separation membranes, it is important to consider that pore clogging can reduce surface area after synthesis and modification with functional groups. The challenge lies in developing multifunctional porous polymers that can effectively maintain a uniform distribution of active sites while preserving porosity. The loading space, a fundamental characteristic of porous materials, has been successfully employed to load the catalysts, electrolytes, biological cells, or drugs for specific applications. Further research on the relationship between the loaded active substances and the physicochemical properties of the raw polymer and pore structure is a desired goal. Certainly, this review only covers a portion of the applications we touched, many valuable emerging fields such as adhesion of wet interfaces and gas dissolution in liquid, could also consider utilizing porous polymers as a useful option to improve their operational performances.

Despite decades of rapid development in the field of porous polymers, this field still encounters severe issues concerning structural stability under adverse circumstances such as high temperature, high humidity, or long-term mechanical stress and fatigue. Strategies such as surface coating, chemical modification, molecular crosslinking, or doping with stabilizer, might improve the stability of porous polymers against environmental factors. In terms of large-scale production, achieving consistent porous structures remains a challenge. Precise control over parameters such as temperature, pressure, material purity, and other factors during the pore formation process is essential for standardizing production and ensuring structural uniformity. Moreover, compatibility issues may arise when porous polymers are integrated with other materials or components. These include insufficient interface bonding strength and mismatches in the thermal expansion coefficient. Addressing these challenges requires interdisciplinary collaboration among materials scientists, mechanical engineers, and other professionals. Such collaboration is crucial for resolving compatibility issues, promoting innovative applications, and advancing technology integration. This paper only scratches the surface of the study of porous polymers. As research progresses, we anticipate that porous polymers with new functionalities will continue to attract interest and find practical applications in various areas.

Author contributions

Q. Liu, and Z. Liu conceived the review and wrote the manuscript. Q. Wang and C. F. Guo reviewed the manuscript and provided the modification suggestions. J. Xiong, W. Lin, J. Liu, and Y. Wan supervised the review and finalized the manuscript. All authors have given approval to the final version of the article.

Data availability

No primary research results or code have been included and no new data were generated or analyzed as part of this review.

Conflicts of interest

The authors declare no conflict of interest.

Acknowledgements

This work was financially supported by the funds of the National Natural Science Foundation of China (no. 52303320, 62205315, 62475250), the STU Scientific Research Foundation for Talents (NTF22035), the General Program of Natural Science Foundation of Guangdong Province (2024A1515010134). The authors also thank the support of ''The Science and Technology Special Foundation Project of Guangdong Province'' (grant no. 210715155861712/2021010201).

References

1 A. G. Slater and A. I. Cooper, *Science*, 2015, **348**, aaa8075.
2 T. D. Bennett, F.-X. Coudert, S. L. James and A. I. Cooper, *Nat. Mater.*, 2021, **20**, 1179–1187.
3 H. M. El-Kaderi, J. R. Hunt, J. L. Mendoza-Cortés, A. P. Côté, R. E. Taylor, M. O'Keeffe and O. M. Yaghi, *Science*, 2007, **316**, 268–272.
4 A. G. Slater and A. I. Cooper, *Science*, 2015, **348**, aaa8075.
5 P. Nugent, Y. Belmabkhout, S. D. Burd, A. J. Cairns, R. Luebke, K. Forrest, T. Pham, S. Ma, B. Space, L. Wojtas, M. Eddaoudi and M. J. Zaworotko, *Nature*, 2013, **495**, 80–84.
6 D. P. Erdosy, M. B. Wenny, J. Cho, C. DelRe, M. V. Walter, F. Jiménez-Ángeles, B. Qiao, R. Sanchez, Y. Peng, B. D. Polizzotti, M. O. De La Cruz and J. A. Mason, *Nature*, 2022, **608**, 712–718.
7 X. Wu, X. Han, Y. Liu, Y. Liu and Y. Cui, *J. Am. Chem. Soc.*, 2018, **140**(47), 16124–16133.
8 J.-K. Sun, M. Antonietti and J. Yuan, *Chem. Soc. Rev.*, 2016, **45**, 6627–6656.
9 L. Tan and B. Tan, *Chem. Soc. Rev.*, 2017, **46**, 3322–3356.
10 H. Sehaqui, Q. Zhou, O. Ikkala and L. A. Berglund, *Biomacromolecules*, 2011, **12**, 3638–3644.
11 J. Zhao, G. Wang, C. Wang and C. B. Park, *Compos. Sci. Technol.*, 2020, **191**, 108084.
12 P. M. Budd, B. S. Ghanem, S. Makhseed, N. B. McKeown, K. J. Msayib and C. E. Tattershall, *Chem. Commun.*, 2004, 230–231.
13 R. M. Allaf, *Funct. 3D Tissue Eng. Scaffolds*, Elsevier, 2018, pp. 75–100.
14 L. Yang, J. Wei, Z. Ma, P. Song, J. Ma, Y. Zhao, Z. Huang, M. Zhang, F. Yang and X. Wang, *Nanomaterials*, 2019, **9**, 1789.
15 Q. Zhao, J. W. C. Dunlop, X. Qiu, F. Huang, Z. Zhang, J. Heyda, J. Dzubiella, M. Antonietti and J. Yuan, *Nat. Commun.*, 2014, **5**, 4293.
16 H. Chen, Z.-G. Gu and J. Zhang, *J. Am. Chem. Soc.*, 2022, **144**(16), 7245–7252.
17 W. Gu, G. Wang, M. Zhou, T. Zhang and G. Ji, *ACS Appl. Mater. Interfaces*, 2020, **12**, 48246–48258.
18 Y. Huang, T. Gancheva, B. D. Favis, A. Abidli, J. Wang and C. B. Park, *ACS Appl. Mater. Interfaces*, 2021, **13**, 16859–16868.
19 B. Zhao, M. Hamidinejad, S. Wang, P. Bai, R. Che, R. Zhang and C. B. Park, *J. Mater. Chem. A*, 2021, **9**, 8896–8949.
20 K. Gong, K. Zhou, X. Qian, C. Shi and B. Yu, *Composites, Part B*, 2021, **217**, 108867.
21 S. Beg, M. Rahman, A. Jain, S. Saini, P. Midoux, C. Pichon, F. J. Ahmad and S. Akhter, *Drug Discovery Today*, 2017, **22**, 625–637.
22 M. Carta, R. Malpass-Evans, M. Croad, Y. Rogan, J. C. Jansen, P. Bernardo, F. Bazzarelli and N. B. McKeown, *Science*, 2013, **339**, 303–307.
23 Y. Xie, T.-T. Wang, X.-H. Liu, K. Zou and W.-Q. Deng, *Nat. Commun.*, 2013, **4**, 1960.
24 M. D. Hager, B. Esser, X. Feng, W. Schuhmann, P. Theato and U. S. Schubert, *Adv. Mater.*, 2020, **32**, 2000587.
25 N. Singh, S. Son, J. An, I. Kim, M. Choi, N. Kong, W. Tao and J. S. Kim, *Chem. Soc. Rev.*, 2021, **50**, 12883–12896.
26 R. M. Spriggs, *J. Am. Ceram. Soc.*, 1961, **44**, 628–629.
27 M. Chen, B. Coasne, R. Guyer, D. Derome and J. Carmeliet, *J. Phys. Chem. B*, 2020, **124**, 8690–8703.
28 Y. Jin, Y. Hu and W. Zhang, *Nat. Rev. Chem.*, 2017, **1**, 0056.
29 L. Zou, Y. Sun, S. Che, X. Yang, X. Wang, M. Bosch, Q. Wang, H. Li, M. Smith, S. Yuan, Z. Perry and H. Zhou, *Adv. Mater.*, 2017, **29**, 1700229.
30 Q. Liu, Y. Liu, J. Shi, Z. Liu, Q. Wang and C. F. Guo, *Nano-Micro Lett.*, 2022, **14**, 21.
31 B. Wicklein, A. Kocjan, G. Salazar-Alvarez, F. Carosio, G. Camino, M. Antonietti and L. Bergström, *Nat. Nanotechnol.*, 2015, **10**, 277–283.
32 B. Khalid, X. Bai, H. Wei, Y. Huang, H. Wu and Y. Cui, *Nano Lett.*, 2017, **17**, 1140–1148.
33 H. Sai, K. W. Tan, K. Hur, E. Asenath-Smith, R. Hovden, Y. Jiang, M. Riccio, D. A. Muller, V. Elser, L. A. Estroff, S. M. Gruner and U. Wiesner, *Science*, 2013, **341**, 530–534.
34 B. Li, Y. Zhang, D. Ma, Z. Xing, T. Ma, Z. Shi, X. Ji and S. Ma, *Chem. Sci.*, 2016, **7**, 2138–2144.
35 K. Pang, X. Liu, J. Pang, A. Samy, J. Xie, Y. Liu, L. Peng, Z. Xu and C. Gao, *Adv. Mater.*, 2022, **34**, 2103740.

36 H. S. Kim, J. Jang, H. Lee, S. Y. Kim, S. H. Kim, J. Kim, Y. C. Jung and B. J. Yang, *Adv. Eng. Mater.*, 2018, **20**, 1800204.
37 S. Liu, S. Qin, Y. Jiang, P. Song and H. Wang, *Composites, Part A*, 2021, **145**, 106376.
38 Y. Sun, Y. Sun, Q. Pan, G. Li, B. Han, D. Zeng, Y. Zhang and H. Cheng, *Chem. Commun.*, 2016, **52**, 3000.
39 B. Yoon, E. Lee, H. Kim and Y. Koh, *J. Am. Ceram. Soc.*, 2007, **90**, 1753–1759.
40 Y. Feng, D. Zong, Y. Hou, X. Yin, S. Zhang, L. Duan, Y. Si, Y. Jia and B. Ding, *J. Colloid Interface Sci.*, 2021, **593**, 59–66.
41 Z. Chen, C. Xu, C. Ma, W. Ren and H. Cheng, *Adv. Mater.*, 2013, **25**, 1296–1300.
42 Y. Cui, H. Gong, Y. Wang, D. Li and H. Bai, *Adv. Mater.*, 2018, **30**, 1706807.
43 J. Mandal, Y. Fu, A. C. Overvig, M. Jia, K. Sun, N. N. Shi, H. Zhou, X. Xiao, N. Yu and Y. Yang, *Science*, 2018, **362**, 315–319.
44 L. Zhao, L. Wang, J. Shi, X. Hou, Q. Wang, Y. Zhang, Y. Wang, N. Bai, J. Yang, J. Zhang, B. Yu and C. F. Guo, *ACS Nano*, 2021, **15**, 5752–5761.
45 X. Zhao, P. Pachfule, S. Li, T. Langenhahn, M. Ye, C. Schlesiger, S. Praetz, J. Schmidt and A. Thomas, *J. Am. Chem. Soc.*, 2019, **141**, 6623–6630.
46 P. X. Ma, *Adv. Drug Delivery Rev.*, 2008, **60**, 184–198.
47 J. Wan, J. Xie, X. Kong, Z. Liu, K. Liu, F. Shi, A. Pei, H. Chen, W. Chen, J. Chen, X. Zhang, L. Zong, J. Wang, L.-Q. Chen, J. Qin and Y. Cui, *Nat. Nanotechnol.*, 2019, **14**, 705–711.
48 Y. Zhao, Y. Sun, X. Xie, Y. Liang, E. A. Cavalcanti-Adam and W. Feng, *Adv. Mater.*, 2024, **36**, 2306814.
49 C. Liu, P.-C. Hsu, H.-W. Lee, M. Ye, G. Zheng, N. Liu, W. Li and Y. Cui, *Nat. Commun.*, 2015, **6**, 6205.
50 S. Karan, Z. Jiang and A. G. Livingston, *Science*, 2015, **348**, 1347–1351.
51 L. Yang, H. Xiao, Y. Qian, X. Zhao, X.-Y. Kong, P. Liu, W. Xin, L. Fu, L. Jiang and L. Wen, *Nat. Sustain.*, 2021, **5**, 71–80.
52 J. R. Holst and A. I. Cooper, *Adv. Mater.*, 2010, **22**, 5212–5216.
53 Z. Li and Y. Yang, *Adv. Mater.*, 2022, **34**, 2107401.
54 B. Dhandayuthapani, Y. Yoshida, T. Maekawa and D. S. Kumar, *Int. J. Polym. Sci.*, 2011, **2011**, 1–19.
55 J. D. Kretlow and A. G. Mikos, *AIChE J.*, 2008, **54**, 3048–3067.
56 W. Bae, H. N. Kim, D. Kim, S. Park, H. E. Jeong and K. Suh, *Adv. Mater.*, 2014, **26**, 675–700.
57 J. Lee and I. Jung, *Appl. Acoust.*, 2019, **151**, 10–21.
58 Z. Zeng, H. Jin, M. Chen, W. Li, L. Zhou and Z. Zhang, *Adv. Funct. Mater.*, 2016, **26**, 303–310.
59 S. Wan, J. Guo, J. Kim, H. Ihee and D. Jiang, *Angew. Chem., Int. Ed.*, 2009, **48**, 5439–5442.
60 W. A. Phillip, Ma. A. Hillmyer and E. L. Cussler, *Macromolecules*, 2010, **43**, 7763–7770.
61 Q. Liu, P. Zhang, B. Na, R. Lv and R. Tian, *J. Phys. Chem. C*, 2014, **118**, 25620–25625.
62 L. J. Gibson and M. F. Ashby, *Cellular Solids: Structure and Properties*, Cambridge University Press, 1997.
63 B. Xie, W. Zhao, X. Luo and R. Hu, *Mater. Sci. Eng., R*, 2023, **154**, 100738.
64 J. F. Van Humbeck, T. M. McDonald, X. Jing, B. M. Wiers, G. Zhu and J. R. Long, *J. Am. Chem. Soc.*, 2014, **136**, 2432–2440.
65 N. Bhardwaj and S. C. Kundu, *Biotechnol. Adv.*, 2010, **28**, 325–347.
66 D. Li and Y. Xia, *Adv. Mater.*, 2004, **16**, 1151–1170.
67 H. Bai, C. Du, A. Zhang and L. Li, *Angew. Chem., Int. Ed.*, 2013, **52**, 12240–12255.
68 G. Shao, D. A. H. Hanaor, X. Shen and A. Gurlo, *Adv. Mater.*, 2020, **32**, 1907176.
69 T. Zhang, R. A. Sanguramath, S. Israel and M. S. Silverstein, *Macromolecules*, 2019, **52**, 5445–5479.
70 L. Tan and B. Tan, *Polym. Chem.*, 2021, **12**, 2689–2694.
71 C. Li, Q. Li, Y. V. Kaneti, D. Hou, Y. Yamauchi and Y. Mai, *Chem. Soc. Rev.*, 2020, **49**, 4681–4736.
72 F. Wang, P. Altschuh, L. Ratke, H. Zhang, M. Selzer and B. Nestler, *Adv. Mater.*, 2019, **31**, 1806733.
73 X.-B. Wang, X.-F. Jiang and Y. Bando, *Bull. Chem. Soc. Jpn.*, 2019, **92**, 245–263.
74 R. Hufenus, Y. Yan, M. Dauner and T. Kikutani, *Materials*, 2020, **13**, 4298.
75 Y. Gao, J. Lalevée and A. Simon-Masseron, *Adv. Mater. Technol.*, 2023, **8**, 2300377.
76 J. Lin, Z. Peng, Y. Liu, F. Ruiz-Zepeda, R. Ye, E. L. G. Samuel, M. J. Yacaman, B. I. Yakobson and J. M. Tour, *Nat. Commun.*, 2014, **5**, 5714.
77 S. Liu, F. Wang, R. Dong, T. Zhang, J. Zhang, X. Zhuang, Y. Mai and X. Feng, *Adv. Mater.*, 2016, **28**, 8365–8370.
78 K.-Y. Chan, X. Shen, J. Yang, K.-T. Lin, H. Venkatesan, E. Kim, H. Zhang, J.-H. Lee, J. Yu, J. Yang and J.-K. Kim, *Nat. Commun.*, 2022, **13**, 5553.
79 Y. Li, J. Zhu, H. Cheng, G. Li, H. Cho, M. Jiang, Q. Gao and X. Zhang, *Adv. Mater. Technol.*, 2021, **6**, 2100410.
80 S. Shi, Y. Si, Y. Han, T. Wu, M. I. Iqbal, B. Fei, R. K. Y. Li, J. Hu and J. Qu, *Adv. Mater.*, 2022, **34**, 2107938.
81 T. D. Brown, P. D. Dalton and D. W. Hutmacher, *Prog. Polym. Sci.*, 2016, **56**, 116–166.
82 T. M. Robinson, D. W. Hutmacher and P. D. Dalton, *Adv. Funct. Mater.*, 2019, **29**, 1904664.
83 T. D. Brown, P. D. Dalton and D. W. Hutmacher, *Adv. Mater.*, 2011, **23**, 5651–5657.
84 D. Li, Y. Wang and Y. Xia, *Nano Lett.*, 2003, **3**, 1167–1171.
85 P. Zhang, R. Tian, B. Na, R. Lv and Q. Liu, *Polymer*, 2015, **60**, 221–227.
86 H. Na, P. Chen, S.-C. Wong, S. Hague and Q. Li, *Polymer*, 2012, **53**, 2736e2743.
87 S. A. Theron, A. L. Yarin, E. Zussman and E. Kroll, *Polymer*, 2005, **46**, 2889–2899.
88 D. Lukas, A. Sarkar and P. Pokorny, *J. Appl. Phys.*, 2008, **103**, 084309.

89 X. Yan, J. Marini, R. Mulligan, A. Deleault, U. Sharma, M. P. Brenner, G. C. Rutledge, T. Freyman and Q. P. Pham, *PLoS One*, 2015, **10**, e0125407.
90 W. E. Teo and S. Ramakrishna, *Nanotechnology*, 2006, **17**, R89–R106.
91 J. Zhao, Y. Li, J. Sheng, X. Wang, L. Liu, J. Yu and B. Ding, *ACS Appl. Mater. Interfaces*, 2017, **9**, 29302–29310.
92 H. Yuan, Q. Zhou and Y. Zhang, *Electrospun Nanofibers*, Elsevier, 2017, pp. 125–147.
93 D. Li, Y. Wang and Y. Xia, *Adv. Mater.*, 2004, **16**, 361–366.
94 X. Wang, B. Ding and B. Li, *Mater. Today*, 2013, **16**, 229–241.
95 J. Wu and Y. Hong, *Bioact. Mater.*, 2016, **1**, 56–64.
96 D. Miao, X. Wang, J. Yu and B. Ding, *Adv. Funct. Mater.*, 2021, **31**, 2008705.
97 S.-F. Chou, D. Carson and K. A. Woodrow, *J. Controlled Release*, 2015, **220**, 584–591.
98 A. Chinnappan, C. Baskar, S. Baskar, G. Ratheesh and S. Ramakrishna, *J. Mater. Chem. C*, 2017, **5**, 12657–12673.
99 F. Zhou, R. Gong and I. Porat, *Polym. Int.*, 2009, **58**, 331–342.
100 X. Li, L. Zhang, Y. Wang, X. Yang, N. Zhao, X. Zhang and J. Xu, *J. Am. Chem. Soc.*, 2011, **133**, 3736–3739.
101 U. H. F. Bunz, *Adv. Mater.*, 2006, **18**, 973–989.
102 M. Srinivasarao, D. Collings, A. Philips and S. Patel, *Sci. New Ser.*, 2001, **292**, 79–83.
103 J. Ding, A. Zhang, H. Bai, L. Li, J. Li and Z. Ma, *Soft Matter*, 2013, **9**, 506–514.
104 L.-S. Wan, J.-W. Li, B.-B. Ke and Z.-K. Xu, *J. Am. Chem. Soc.*, 2012, **134**, 95–98.
105 L. A. Connal and G. G. Qiao, *Soft Matter*, 2007, **3**, 837–839.
106 J. S. Park, S. H. Lee, T. H. Han and S. O. Kim, *Adv. Funct. Mater.*, 2007, **17**, 2315–2320.
107 M. H. Stenzel, C. Barner-Kowollik and T. P. Davis, *J. Polym. Sci., Part A: Polym. Chem.*, 2006, **44**, 2363–2375.
108 P. Escalé, L. Rubatat, L. Billon and M. Save, *Eur. Polym. J.*, 2012, **48**, 1001–1025.
109 R. Dong, J. Yan, H. Ma, Y. Fang and J. Hao, *Langmuir*, 2011, **27**, 9052–9056.
110 G. Lu, W. Li, J. Yao, G. Zhang, B. Yang and J. Shen, *Adv. Mater.*, 2002, **14**, 1049–1053.
111 X. Jiang, T. Zhang, L. Xu, C. Wang, X. Zhou and N. Gu, *Langmuir*, 2011, **27**, 5410–5419.
112 F.-L. Jin, M. Zhao, M. Park and S.-J. Park, *Polymers*, 2019, **11**, 953.
113 X.-B. Wang, X.-F. Jiang and Y. Bando, *Bull. Chem. Soc. Jpn.*, 2019, **92**, 245–263.
114 C. Okolieocha, D. Raps, K. Subramaniam and V. Altstädt, *Eur. Polym. J.*, 2015, **73**, 500–519.
115 J. S. Colton and N. P. Suh, *Polym. Eng. Sci.*, 1987, **27**, 485–492.
116 Y. W. Chen, H. Zhan and J. N. Wang, *Nanoscale*, 2021, **13**, 11878–11886.
117 H. Wang, R. Zhang, D. Yuan, S. Xu and L. Wang, *Adv. Funct. Mater.*, 2020, **30**, 2003995.
118 L. J. M. Jacobs, K. C. H. Danen, M. F. Kemmere and J. T. F. Keurentjes, *Polymer*, 2007, **48**, 3771e3780.
119 S.-T. Lee, C. B. Park and N. S. Ramesh, *Polymeric foams: science and technology*, CRC Press, 2006.
120 S. Loeb and S. Sourirajan, *Saline Water Conversion-II*, AMerican Chemical Society, Washington, DC, 1963.
121 M. Müller and V. Abetz, *Chem. Rev.*, 2021, **121**, 14189–14231.
122 K. V. Pochivalov, A. V. Basko, T. N. Lebedeva, A. N. Ilyasova, M. Y. Yurov, R. Y. Golovanov, V. V. Artemov, V. V. Volkov, A. A. Ezhov, A. V. Volkov and Y. V. Kudryavtsev, *Mater. Today Commun.*, 2021, **28**, 102558.
123 G. R. Guillen, Y. Pan, M. Li and E. M. V. Hoek, *Ind. Eng. Chem. Res.*, 2011, **50**, 3798–3817.
124 P. V. D. Witte, H. Esselbrugge, P. J. Dijkstra, J. W. A. Van Den Berg and J. Feijen, *J. Polym. Sci., Polym. Phys. Ed.*, 1996, **34**, 2569–2578.
125 Q. Liu, R. Lv, B. Na and Y. Ju, *RSC Adv.*, 2015, **5**, 57076–57081.
126 R. Liu, K. Li, M. Liu, Y. Liu and H. Liu, *J. Polym. Sci., Part B: Polym. Phys.*, 2014, **52**, 1476–1489.
127 O. C. Onder, E. Yilgor and I. Yilgor, *Polym. Sci.*, 2019, **57**, 98–108.
128 G. Shao, D. A. H. Hanaor, X. Shen and A. Gurlo, *Adv. Mater.*, 2020, **32**, 1907176.
129 H. Bai, Y. Chen, B. Delattre, A. P. Tomsia and R. O. Ritchie, *Sci. Adv.*, 2015, **1**, e1500849.
130 W. Xu, Y. Xing, J. Liu, H. Wu, Y. Cui, D. Li, D. Guo, C. Li, A. Liu and H. Bai, *ACS Nano*, 2019, **13**, 7930–7938.
131 H. Xiao, X. Zhao, J. Lv, X. He, M. Chen, W. Tan, W. Yang, K. Zeng, J. Hu and G. Yang, *Polym. Eng. Sci.*, 2023, **63**, 3819–3830.
132 H. Xiao, J. Lv, W. Tan, X. He, M. Chen, K. Zeng, J. Hu and G. Yang, *Chem. Eng. J.*, 2022, **450**, 138344.
133 Y. Zhang, L. Hu and J. Han, *J. Am. Ceram. Soc.*, 2009, **92**, 1874–1876.
134 I. Nelson, T. A. Ogden, S. Al Khateeb, J. Graser, T. D. Sparks, J. J. Abbott and S. E. Naleway, *Adv. Eng. Mater.*, 2019, **21**, 1801092.
135 H. Janik and M. Marzec, *Mater. Sci. Eng., C*, 2015, **48**, 586–591.
136 C. Li, Q. Li, Y. V. Kaneti, D. Hou, Y. Yamauchi and Y. Mai, *Chem. Soc. Rev.*, 2020, **49**, 4681–4736.
137 S. Kandambeth, V. Venkatesh, D. B. Shinde, S. Kumari, A. Halder, S. Verma and R. Banerjee, *Nat. Commun.*, 2015, **6**, 6786.
138 Q. Li, J. F. Quinn and F. Caruso, *Adv. Mater.*, 2005, **17**, 2058–2062.
139 M. Stucki, M. Loepfe and W. J. Stark, *Adv. Eng. Mater.*, 2017, **20**, 1700611.
140 S. A. Bencherif, T. M. Braschler and P. Renaud, *J. Periodontal Implant Sci.*, 2013, **43**, 251.
141 Y.-Y. Liu, X.-C. Li, S. Wang, T. Cheng, H. Yang, C. Liu, Y. Gong, W.-Y. Lai and W. Huang, *Nat. Commun.*, 2020, **11**, 5561.
142 R. W. Jaggers, R. Chen and S. A. F. Bon, *Mater. Horiz.*, 2016, **3**, 41–46.
143 L. J. Tan, W. Zhu and K. Zhou, *Adv. Funct. Mater.*, 2020, **30**, 2003062.

144 X. Zheng, W. Smith, J. Jackson, B. Moran, H. Cui, D. Chen, J. Ye, N. Fang, N. Rodriguez, T. Weisgraber and C. M. Spadaccini, *Nat. Mater.*, 2016, **15**, 1100–1106.
145 K. K. Phani and S. K. Niyogi, *J. Mater. Sci.*, 1987, **22**, 257–263.
146 U. Pierre Claver and G. Zhao, *Adv. Eng. Mater.*, 2021, **23**, 2001187.
147 S. Lee, S. Franklin, F. A. Hassani, T. Yokota, O. G. Nayeem, Y. Wang, R. Leib, G. Cheng, D. W. Franklin and T. Someya, *Science*, 2020, **370**, 966–970.
148 S. R. A. Ruth, V. R. Feig and H. Tran, *Adv. Funct. Mater.*, 2020, **30**, 2003491.
149 Y. Huang, X. Fan, S.-C. Chen and N. Zhao, *Adv. Funct. Mater.*, 2019, **29**, 1808509.
150 H.-B. Yao, J. Ge, C.-F. Wang, X. Wang, W. Hu, Z.-J. Zheng, Y. Ni and S.-H. Yu, *Adv. Mater.*, 2013, **25**, 6692–6698.
151 D. Chen, M. Hang, K. Chen, K. Brown and J. X. J. Zhang, *2015 IEEE Sens*, IEEE, Busan, 2015, pp. 1–4.
152 K. Y. Lee, J. Chun, J. Lee, K. N. Kim, N. Kang, J. Kim, M. H. Kim, K. Shin, M. K. Gupta, J. M. Baik and S. Kim, *Adv. Mater.*, 2014, **26**, 5037–5042.
153 S. C. B. Mannsfeld, B. C.-K. Tee, R. M. Stoltenberg, C. V. H.-H. Chen, S. Barman, B. V. O. Muir, A. N. Sokolov, C. Reese and Z. Bao, *Nat. Mater.*, 2010, **9**, 859–864.
154 Y. Wan, Z. Qiu, Y. Hong, Y. Wang, J. Zhang, Q. Liu, Z. Wu and C. F. Guo, *Adv. Electron. Mater.*, 2018, **4**, 1700586.
155 Y. Zhang, X. Zhou, N. Zhang, J. Zhu, N. Bai, X. Hou, T. Sun, G. Li, L. Zhao, Y. Chen, L. Wang and C. F. Guo, *Nat. Commun.*, 2024, **15**, 3048.
156 Y. Zhang, J. Yang, X. Hou, G. Li, L. Wang, N. Bai, M. Cai, L. Zhao, Y. Wang, J. Zhang, K. Chen, X. Wu, C. Yang, Y. Dai, Z. Zhang and C. F. Guo, *Nat. Commun.*, 2022, **13**, 1317.
157 R. Li, Y. Si, Z. Zhu, Y. Guo, Y. Zhang, N. Pan, G. Sun and T. Pan, *Adv. Mater.*, 2017, **29**, 1700253.
158 R. Li, B. Nie, C. Zhai, J. Cao, J. Pan, Y.-W. Chi and T. Pan, *Ann. Biomed. Eng.*, 2016, **44**, 2282–2291.
159 Y. Chang, L. Wang, R. Li, Z. Zhang, Q. Wang, J. Yang, C. F. Guo and T. Pan, *Adv. Mater.*, 2020, **33**, 2003464.
160 J. A. Greenwood and J. B. P. Williamson, *Proc. R. Soc. London, Ser. A*, 1966, **295**, 300–319.
161 K. L. Johnson, *Proc. - Inst. Mech. Eng.*, 1982, **196**, 363–378.
162 N. Bai, L. Wang, Q. Wang, J. Deng, Y. Wang, P. Lu, J. Huang, G. Li, Y. Zhang, J. Yang, K. Xie, X. Zhao and C. F. Guo, *Nat. Commun.*, 2020, **11**, 209.
163 Y. Wan, Z. Qiu, J. Yuan, J. Yang, J. Li and C. F. Guo, *J. Phys. D: Appl. Phys.*, 2023, **57**, 093002.
164 A. S. Fiorillo, C. D. Critello1 and S. A. Pullano, *Sens. Actuators, A*, 2018, **281**, 156–175.
165 J. He, Y. Zhang, R. Zhou, L. Meng, C. Pan, W. Mai, T. Chen, W. Mai and C. Pan, *J. Materiomics*, 2020, **6**, 86–101.
166 C.-L. Choong, M.-B. Shim, B.-S. Lee, S. Jeon, D.-S. Ko, T.-H. Kang, J. Bae, S. H. Lee, K.-E. Byun, J. Im, Y. J. Jeong, C. E. Park, J.-J. Park and U.-I. Chung, *Adv. Mater.*, 2014, **26**, 3451–3458.
167 L. Pan, A. Chortos, G. Yu, Y. Wang, S. Isaacson, R. Allen, Y. Shi, R. Dauskardt and Z. Bao, *Nat. Commun.*, 2014, **5**, 3002.
168 Y. Yang, H. Pan, G. Xie, Y. Jiang, C. Chen, Y. Su, Y. Wang and H. Tai, *Sens. Actuators, A*, 2020, **301**, 111789.
169 N. Chamankar, R. Khajavi, A. A. Yousefi, A. Rashidi and F. Golestanifard, *Ceram. Int.*, 2020, **46**, 19669–19681.
170 Y. R. Wang, J. M. Zheng, G. Y. Ren, P. H. Zhang and C. Xu, *Smart Mater. Struct.*, 2011, **20**, 045009.
171 C. Lv, Z. Zhou, Y. Li, S. Lu and Y. Bai, *Chem. Eng. J.*, 2023, **477**, 147059.
172 B. Yu, H. Yu, H. Wang, Q. Zhang and M. Zhu, *Nano Energy*, 2017, **34**, 69–75.
173 K. Dong, X. Peng, J. An, A. C. Wang, J. Luo, B. Sun, J. Wang and Z. L. Wang, *Nat. Commun.*, 2020, **11**, 2868.
174 I. Sumirat, Y. Ando and S. Shimamura, *J. Porous Mater.*, 2006, **13**, 439–443.
175 A. Fraleoni-Morgera and M. Chhikara, *Adv. Eng. Mater.*, 2019, **21**, 1801162.
176 F. F. Ling, *Principles of Heat Transfer in Porous Media*, Springer-Verlag, New York, 1991.
177 V. Apostolopoulou-Kalkavoura, P. Munier and L. Bergström, *Adv. Mater.*, 2021, **33**, 2001839.
178 X. Lu, M. C. Arduini-Schuster, J. Kuhn, O. Nilsson, J. Fricke and R. W. Pekala, *Science*, 1992, **255**, 971–972.
179 B. Wicklein, A. Kocjan, G. Salazar-Alvarez, F. Carosio, G. Camino, M. Antonietti and L. Bergström, *Nat. Nanotechnol.*, 2015, **10**, 277–283.
180 W. Fan, X. Zhang, Y. Zhang, Y. Zhang and T. Liu, *Compos. Sci. Technol.*, 2019, **173**, 47–52.
181 T. Wang, Y. Wu, L. Shi, X. Hu, M. Chen and L. Wu, *Nat. Commun.*, 2021, **12**, 365.
182 W. Zhu, B. Droguet, Q. Shen, Y. Zhang, T. G. Parton, X. Shan, R. M. Parker, M. F. L. De Volder, T. Deng, S. Vignolini and T. Li, *Adv. Sci.*, 2022, **9**, 2202061.
183 J. Li, Y. Liang, W. Li, N. Xu, B. Zhu, Z. Wu, X. Wang, S. Fan, M. Wang and J. Zhu, *Sci. Adv.*, 2022, **8**, eabj9756.
184 P.-C. Hsu, A. Y. Song, P. B. Catrysse, C. Liu, Y. Peng, J. Xie, S. Fan and Y. Cui, *Science*, 2016, **353**, 1019–1023.
185 L. Zhou, Y. Tan, D. Ji, B. Zhu, P. Zhang, J. Xu, Q. Gan, Z. Yu and J. Zhu, *Sci. Adv.*, 2016, **2**, e1501227.
186 C. Chen, Y. Kuang and L. Hu, *Joule*, 2019, **3**, 683–718.
187 G. Ni, G. Li, S. V. Boriskina, H. Li, W. Yang, T. Zhang and G. Chen, *Nat. Energy*, 2016, **1**, 16126.
188 F. Shahzad, M. Alhabeb, C. B. Hatter, B. Anasori, S. Man Hong, C. M. Koo and Y. Gogotsi, *Science*, 2016, **353**, 1137–1140.
189 T. Yun, H. Kim, A. Iqbal, Y. S. Cho, G. S. Lee, M. Kim, S. J. Kim, D. Kim, Y. Gogotsi, S. O. Kim and C. M. Koo, *Adv. Mater.*, 2020, **32**, 1906769.
190 D. Jiang, V. Murugadoss, Y. Wang, J. Lin, T. Ding, Z. Wang, Q. Shao, C. Wang, H. Liu, N. Lu, R. Wei, A. Subramania and Z. Guo, *Polym. Rev.*, 2019, **59**, 280–337.
191 A. Iqbal, F. Shahzad, K. Hantanasirisakul, M.-K. Kim, J. Kwon, J. Hong, H. Kim, D. Kim, Y. Gogotsi and C. M. Koo, *Science*, 2020, **369**, 446–450.

192 Y. Cheng, X. Li, Y. Qin, Y. Fang, G. Liu, Z. Wang, J. Matz, P. Dong, J. Shen and M. Ye, *Sci. Adv.*, 2021, **7**, eabj1663.
193 Y. Chen, Y. Yang, Y. Xiong, L. Zhang, W. Xu, G. Duan, C. Mei, S. Jiang, Z. Rui and K. Zhang, *Nano Today*, 2021, **38**, 101204.
194 Q. Song, F. Ye, L. Kong, Q. Shen, L. Han, L. Feng, G. Yu, Y. Pan and H. Li, *Adv. Funct. Mater.*, 2020, **30**, 2000475.
195 N. Yousefi, X. Sun, X. Lin, X. Shen, J. Jia, B. Zhang, B. Tang, M. Chan and J. Kim, *Adv. Mater.*, 2014, **26**, 5480–5487.
196 J. Feng, Z. Zhuang, Y. Zhou and C. Li, *Adv. Funct. Mater.*, 2024, 2315188.
197 Z. Zeng, F. Jiang, Y. Yue, D. Han, L. Lin, S. Zhao, Y. Zhao, Z. Pan, C. Li, G. Nyström and J. Wang, *Adv. Mater.*, 2020, **32**, 1908496.
198 Y. Wan, P. Xiong, J. Liu, F. Feng, X. Xun, F. M. Gama, Q. Zhang, F. Yao, Z. Yang, H. Luo and Y. Xu, *ACS Nano*, 2021, **15**, 8439–8449.
199 M. Liang, H. Wu, J. Liu, Y. Shen and G. Wu, *J. Porous Mater.*, 2022, **29**, 869–892.
200 M. A. Kuczmarski and J. C. Johnston, *NASA/TM*, 2011, 216995.
201 K. Attenborough, *Phys. Rep.*, 1982, **82**, 179–227.
202 J. P. Arenas and M. J. Crocker, *Sound Vib.*, 2010, **44**, 12–18.
203 M. Rahimabady, E. C. Statharas, K. Yao, M. Sharifzadeh Mirshekarloo, S. Chen and F. E. H. Tay, *Appl. Phys. Lett.*, 2017, **111**, 241601.
204 K. Pang, X. Liu, J. Pang, A. Samy, J. Xie, Y. Liu, L. Peng, Z. Xu and C. Gao, *Adv. Mater.*, 2022, **34**, 2103740.
205 G.-H. Zhang, Q.-H. Zhu, L. Zhang, F. Yong, Z. Zhang, S.-L. Wang, Y. Wang, L. He and G.-H. Tao, *Nat. Commun.*, 2020, **11**, 1653.
206 J. Xu, C. Liu, P.-C. Hsu, K. Liu, R. Zhang, Y. Liu and Y. Cui, *Nano Lett.*, 2016, **16**, 1270–1275.
207 Z. Shao, H. Chen, Q. Wang, G. Kang, X. Wang, W. Li, Y. Liu and G. Zheng, *Sep. Purif. Technol.*, 2022, **302**, 122175.
208 R. Zhang, C. Liu, P.-C. Hsu, C. Zhang, N. Liu, J. Zhang, H. R. Lee, Y. Lu, Y. Qiu, S. Chu and Y. Cui, *Nano Lett.*, 2016, **16**, 3642–3649.
209 Z. Qiao, S. Zhao, M. Sheng, J. Wang, S. Wang, Z. Wang, C. Zhong and M. D. Guiver, *Nat. Mater.*, 2019, **18**, 163–168.
210 Z. Wang, X. Luo, Z. Song, K. Lu, S. Zhu, Y. Yang, Y. Zhang, W. Fang and J. Jin, *Nat. Commun.*, 2022, **13**, 4169.
211 H. Wang, S. Zhao, Y. Liu, R. Yao, X. Wang, Y. Cao, D. Ma, M. Zou, A. Cao, X. Feng and B. Wang, *Nat. Commun.*, 2019, **10**, 4204.
212 X. Shi, L. Wang, N. Yan, Z. Wang, L. Guo, M. Steinhart and Y. Wang, *The Innovation*, 2021, **2**, 100088.
213 P. Kaur, J. T. Hupp and S. T. Nguyen, *ACS Catal.*, 2011, **1**, 819–835.
214 M. A. Rivero-Crespo, G. Toupalas and B. Morandi, *J. Am. Chem. Soc.*, 2021, **143**, 21331–21339.
215 Q. Sun, Z. Dai, X. Meng and F.-S. Xiao, *Chem. Soc. Rev.*, 2015, **44**, 6018–6034.
216 R. Poupart, D. Grande, B. Carbonnier and B. Le Droumaguet, *Prog. Polym. Sci.*, 2019, **96**, 21–42.
217 F. Wang, J. Mielby, F. H. Richter, G. Wang, G. Prieto, T. Kasama, C. Weidenthaler, H. Bongard, S. Kegnæs, A. Fürstner and F. Schüth, *Angew. Chem., Int. Ed.*, 2014, **53**, 8645.
218 Y. Shi, L. Peng, Y. Ding, Y. Zhao and G. Yu, *Chem. Soc. Rev.*, 2015, **44**, 6684–6696.
219 B. Zheng, X. Lin, X. Zhang, D. Wu and K. Matyjaszewski, *Adv. Funct. Mater.*, 2019, 1907006.
220 X. Liu, C. Liu, W. Lai and W. Huang, *Adv. Mater. Technol.*, 2020, **5**, 2000154.
221 S. Wu, X. Liu, K. W. K. Yeung, C. Liu and X. Yang, *Mater. Sci. Eng., R*, 2014, **80**, 1–36.
222 S. J. Hollister, *Nat. Mater.*, 2005, **4**, 518–524.
223 M. M. Laronda, A. L. Rutz, S. Xiao, K. A. Whelan, F. E. Duncan, E. W. Roth, T. K. Woodruff and R. N. Shah, *Nat. Commun.*, 2017, **8**, 15261.
224 J. Lv, X. Li, H. Yin, L. Wang, Y. Pei and X. Lv, *Chem. Eng. J.*, 2017, **325**, 601–610.
225 Y. Xu, C. Kim, D. M. Saylor and D. Koo, *J. Biomed. Mater. Res, Part B*, 2017, **105**, 1692–1716.
226 V. S. Vyas, M. Vishwakarma, I. Moudrakovski, F. Haase, G. Savasci, C. Ochsenfeld, J. P. Spatz and B. V. Lotsch, *Adv. Mater.*, 2016, **28**, 8749–8754.
227 P. Horcajada, T. Chalati, C. Serre, B. Gillet, C. Sebrie, T. Baati, J. F. Eubank, D. Heurtaux, P. Clayette, C. Kreuz, J.-S. Chang, Y. K. Hwang, V. Marsaud, P.-N. Bories, L. Cynober, S. Gil, G. Férey, P. Couvreur and R. Gref, *Nat. Mater.*, 2010, **9**, 172–178.

